Thesis/
Reports
Wilcock,
P.R.

The Johns Hopkins University

A Method for Predicting Sediment Transport in Gravel-Bed Rivers

Peter R. Wilcock

March 31, 1997

AE30010002

Hopkins

A Method for Predicting Sediment Transport in Gravel-Bed Rivers

Peter R. Wilcock

March 31, 1997

Department of Geography and Environmental Engineering
The Johns Hopkins University
Baltimore Maryland 21218

National FS Library
USDA Forest Service

MAY 16 2011

240 W Prospect Rd
Fort Collins CO 80526

A report prepared in accordance with Partnership Agreement 28-CCS5-019 between the Johns Hopkins University and the U.S. Forest Service Rocky Mountain Forest and Range Experiment Station.

Summary

This report presents a method for predicting transport rates in gravel-bed rivers. Sand and gravel transport rates are predicted separately for the simple reason that the sand and gravel fractions behave differently. There are practical reasons as well: two fractions are the minimum needed to predict changes in grain size in gravel-bed rivers while also requiring input information that may be practically collected in the field.

It has been widely documented that transport in gravel bed rivers is highly variable over a range of scales of space and time. Some of this variability is due to corresponding variation in the flow and sediment. Some is due to inherent instability in the transport process. The variability has two important implications for the type of model that is used to forecast transport. A model that provides a relatively complete prediction of the transport field, including the grain size and rate of transport at a local scale (roughly one m or less), necessarily depends on details of local flow and sediment properties. For practical purposes, however, it is nearly impossible to gather the necessary local input required for such a model. Further, even if such detail were available, it is unlikely that such a model would accurately capture the local transport for more than a short period, after which the inherent instabilities in the transport process cause the local sediment and flow to change. Together, these problems of effort and variability make it unlikely that the accuracy of a detailed "local" transport model will be any better than a forecast based on mean properties of the flow and sediment. Indeed, because transport is a rapidly varying and nonlinear function of the flow, it is quite possible that a local transport model would give less accurate forecasts than a model based on suitably defined mean properties. In this sense, transport in a gravel-bed river is like a powerful but sensitive automobile: in the hands of an ignorant driver (one ignorant of the necessary details of its operation), it is likely to break down, perhaps even crash.

To avoid these problems of accuracy and effort, the method presented here is based on suitably defined mean properties of the flow and sediment in a stream reach. At the same time, it goes beyond predicting a single value of total bed material load and predicts separately the transport rates of the sand and gravel portions of the load. This two-fraction approach captures an important sorting process that produces changes in the grain size of the bed and transport and provides direct application to practical problems such as the maintenance and flushing of river channels and the passage of large quantities of fine sediment introduced to the channel. The field effort required to

implement the two-fraction model is not substantially more difficult than that required for a one-fraction total load calculation.

The basic choices available to forecast transport in gravel-bed rivers have been to either predict it, based on mean properties of the channel reach, or to measure it over the range of flows of interest. Both choices fail on a practical level. The predictive approach fails because of its typically large inaccuracy; the empirical approach fails because of the large amount of work required to establish a reliable sediment rating curve. A compromise is developed here. Transport rates are predicted using the two-fraction model developed in this report. At the same time, a small number of transport observations are used to improve the accuracy of the forecast. The transport samples are used to reduce the error in the term in the transport model (the ratio of the bed shear stress to the critical value of bed shear stress for initial grain motion) that is responsible for most of the error for the range of flows typically observed in gravel-bed rivers. Because the number of transport samples required is small and the samples are obtained at low transport rates, a more accurate transport forecast is possible without the expense and risk associated with a sampling program over the full range of flows.

In this report, the reasoning behind the two-fraction transport model is presented and its specific form is developed from some of the best available transport data. The data requirements for applying the model are then described and a sampling plan for collecting these data is outlined. The model may be applied in a completely predictive form in which transport rates are predicted as a function of the mean bed material size distribution and flow characteristics of a channel reach. Greater accuracy will be achieved if the model is calibrated by using observations of transport at small stages to determine the discharge producing initial motion. The model is then used to predict sand and gravel transport rates at higher stages. Although the second option requires more field work, the effort involved is far less than that needed to determine an entire sediment rating curve from field observations. After the field sites are established, the level of effort required is such that a number of streams may be observed by single person, so that the fieldwork can form the basis of a river monitoring plan.

The method presented here incorporates two concepts whose interrelationship is worth emphasizing: the two fraction transport model and the use of direct observations of small transport rates to improve the accuracy of the calculated transport rate. Although related, these two concepts are independent. The calibrated approach to estimating transport rates may be used with virtually

any transport model (most directly with those models that include a flow parameter representing the onset of sediment motion). Conversely, the two fraction transport model may be used with or without direct calibration. In combination, the two concepts should provide estimates of bed-material transport that are more accurate than otherwise possible, that can estimate changes in bed grain size, and that require field input that may be collected using conventional field techniques.

Type of Model

The model is developed to predict the total bed-material load. A formal distinction is not made between bed load and suspended load. Rather, the objective is to predict the transport rates of material found in the bed. The application is for gravel-bed rivers with a variable sand component. The smallest grain sizes used in the model are assumed to be on the order of one-quarter mm or larger. At high flows, a portion of the finest grains will travel in suspension, although little of the total sand transport may be expected to be dispersed throughout the water column, as would be expected for very fine sand, silt and clay. The focus is on sediment that spends most of its time on or within the bed.

Introduction

A means of calculating sediment transport rate in gravel-bed rivers is needed to determine the flow regime required to maintain the channel, which must transport the sediment supplied to it. The need for accurate transport estimates is balanced by the large amount of work required to develop complete transport rating curves from field measurements and by the number of channels for which transport estimates are potentially required. An approach that provides both sufficient accuracy and a minimum of field effort would have clear benefits. The goal of this work is to develop a method for predicting transport rates in gravel bed rivers that achieves a useful and practical compromise between prediction accuracy and field effort.

In the proposed method, separate predictions are made for the sand and gravel portions of the bed material. A two-part transport relation provides a means of predicting the variation in the fines content of the bed, which is generally more variable than that of the coarse fraction, and whose passage, intrusion, or removal may be a specific objective of channel maintenance flows. A two-part transport relation allows prediction of relatively large sand transport rates at low to moderate flows, a common feature of gravel-bed rivers.

The basic premise of the model is that the transport rates of different sizes within a gravel bed may be represented by two different relations: one for the sand, or matrix, material and one for the gravel, or framework, material. In general, the transport rates of sand and gravel can be predicted with greater accuracy when they are found in separate, well-sorted beds than when combined in widely sorted mixture. This observation, together with the observation that the sand and gravel portions of the bed can behave differently, motivates the particular approach used here: the sand and gravel are assumed to be separate well-behaved populations. It is further assumed that interactions between the two groups are relatively simple and may be consistently described as the proportions of the two change.

There are practical reasons to predict separately the transport rates of sand and gravel. Two size fractions are the minimum needed to forecast any change in the grain size of a river bed. That such a simple approach could represent real size changes of practical significance depends on the distinct behavior of the sand and gravel fractions and the fact that the fines content of a river bed tends to be more transient than the gravel/cobble framework of the bed. The two-fraction approach can predict the change in bed grain size due to changes in the relative proportion of sand and gravel, but not due to the changes in the representative grain size of either fraction. The relevance

of the approach arises from the fact that a number of activities, such as logging, road construction, dam operation, and reservoir maintenance can increase the supply of fine-grained sediment to a river, causing an increase of fines content in the bed, often with detrimental environmental consequences. If the supply of fine sediment can be reduced, removal of the accumulated fines is an important goal. A separate forecast of sand and gravel transport rates is needed to evaluate the flows that may be used to remove the fine sediment and to estimate the time needed to restore the bed.

The method predicts a minimum set of useful properties—the transport rate of the sand and gravel portions of the load—while attempting to balance acceptable prediction accuracy with efficient use of limited resources for collecting field data. The basic information needed to forecast transport rates is comparable to that required to forecast the total bed material load from a transport formula, but is likely to provide more accurate results. The proposed method requires far less effort than that required to predict the transport rates of many individual size fractions from a fractional transport model. If the gravel size distribution is assumed to be less transient than that of the fines, periodic monitoring of the bed and updated transport forecasts may be based on visual surveys of the fines content, which may be determined fairly quickly for large reaches. The result is an updateable prediction of the salient practical features of the transport, using measurable quantities, with acceptable accuracy.

Predicting Bed-Load Transport: Options, Accuracy, Cost

In general, two options exist for predicting bed-material transport in a gravel-bed river. In the first, a formula is used to predict transport rate as a function of average properties of the channel bed and geometry. In the second option, transport is measured directly. Both choices fail on a practical level. The predictive approach fails because of its typically large inaccuracy; the empirical approach fails because of the large amount of work required to establish a reliable sediment rating curve makes application beyond research purposes on a few streams unlikely. A third option is suggested here, in which a few transport observations made at small transport rates are used to improve the accuracy of predictions made with a transport model. Its objective is to preserve the convenience of the predictive approach, while improving its accuracy.

The predictive approach uses any of a number of sediment transport formulas (e.g. Meyer-Peter and Müller, 1948; Ackers and White, 1972; Parker et al., 1982) to predict either the total bedload transport or the transport rate of individual size fractions (fractional transport rate). The information needed is (1) the grain size of the river bed (typically a coarse size such as D_{65} or D_{84} for determining hydraulic roughness and either the median grain size D_{50} for predicting total load or the overall bed size distribution for predicting fractional transport) and (2) the channel geometry of the reach (typically bed slope and the variation of flow depth and cross-sectional area as a function of discharge). From these quantities, dimensionless parameters representing the flow and the sediment are calculated and used with the transport formula to predict the transport rate. Rather than water discharge, transport formulas typically use a more elementary variable for the flow (most commonly the bed shear stress τ_0) because the effectiveness of discharge in moving sediment will vary with channel geometry, planform, and roughness.

Among the many sources of error associated with the predictive approach, the most important is that due to spatial variability in τ_0. Because sediment transport rate varies rapidly with τ_0, even small errors in predicting the flow can produce very large, generally unacceptable, errors in the predicted transport rate. Furthermore, because transport varies with τ_0 in a nonlinear fashion, even an accurate estimate of τ_0 may be poorly correlated with transport rate. This is because the degree by which the transport differs from the section mean will be much larger in areas of large local τ_0 than it will be in areas of small τ_0. (Mathematically, the mean of a power is not equal to the power of a mean, which is the same problem that gives rise to velocity coefficients in one-dimensional channel hydraulics.)

Transport rate is sensitive not only to τ_0, but also to grain size, which also varies spatially in a channel bed. To account for spatial variation in both flow and sediment, it is possible to predict the local flow and transport field throughout a river reach. The total transport rate is then found by cumulating the transport rate across a section. Because the transport rate is sensitive to grain size at any point on the bed, such a modeling effort requires knowledge of the bed grain size and topography throughout a reach. The effort required to determine the input can become very large; this problem becomes intractable when the bed size distribution is subject to change, or when the transport for a number of streams must be forecast. A complete map of the local grain size and topography might be justified if it could be done only once; it would be hard to support making the same effort repeatedly. What is desirable is a means of monitoring the size distribution throughout a reach that does not require extensive and time-consuming sampling.

An empirical relation between transport rate and flow discharge may be developed directly from a large number of observations of the transport rate. In a few research efforts, the entire transport load is caught in a slot or other trap extending across the full width of the river (e.g. Milhous, 1973; Emmett, 1980; Kuhnle, 1992). In practice, a small sampler is used to collect a small portion of the bed-load. Because of the large spatial and temporal variability characteristic of bedload transport, a reliable estimate of the total transport through a section requires a large number of samples (Emmett, 1980). When compounded by the range of flows for which transport observations are needed, the required effort is large.

The empirical approach has the important advantage that the quantity of interest, sediment transport rate, is directly measured. It also has the advantage that the transport rate is directly correlated with the water discharge, which is commonly measured with good accuracy using conventional methods. This avoids the serious problems of predicting the local flow from the discharge, as is needed for most transport models. The tradeoff, of course, is the effort involved and the fact that the sediment rating curve applies to only the measured reach of one stream. Transport predictions from sediment rating curves are not without error, because of sampling error (sampled load not equal to the actual load at the time of sampling) and because of real variations in sediment transport. In the best of cases, uncertainty in the predicted load is not likely to be reduced to less than an order of magnitude.

The method developed here is a compromise between the predictive and empirical approaches. It attempts to strike a balance between the effort (and cost) required to collect field

data and the need to develop accurate estimates of the dominant features of bed-load transport. The transport is predicted using a formula (whether the model presented here or another transport formula). A small number of transport observations at flow conditions producing small transport rates are used to calibrate the predictive model, thereby increasing its accuracy. The goal of the transport observations is to identify the critical shear stress τ_c, which is the value of τ_0 producing incipient transport. Transport models typically contain a term τ_0/τ_c, the uncertainty in which is the dominant source of error in transport predictions. Transport measurements permitting a direct estimate of τ_c reduce the error in τ_0/τ_c, thereby increasing the accuracy of the transport predictions.

The two-fraction transport model offers some additional advantages in terms of field effort. It requires as input the proportion of sand and gravel in the upstream channel. This may be found by visually estimating the proportion of sand on the bed. Areas with similar fines content may be mapped and combined to give a weighted average proportion of sand for the reach. This is far less information than that required for a fractional transport model, and is comparable to the effort required for a total bedload model that uses a characteristic size (e.g. D_{50}) of the bed. If the bed size changes, any of these approaches requires a resurvey. If the change in size is due primarily to the introduction or removal of sand, however, the two-fraction approach requires only a remapping of fines content, a relatively quick procedure compared to the effort required to characterize the grain size of the upstream reach.

The tradeoff between accuracy and effort (or cost) for the three methods may be illustrated schematically (Figure 1). The cost of data collection may be expected to include a fixed cost (e.g. field work to describe the channel reach) and a per-observation cost for bedload sampling (Figure 1a). (A single bedload observation is a single estimate of the total bedload through a section, based on many samples taken across the section.) The predictive model involves only the fixed start-up cost, whereas the empirical and combined methods include both a start-up and per-sample cost.

Prediction accuracy may be defined as $(q_b - \varepsilon)/q_b$, where q_b is transport rate and ε is the error, which can be defined as the expected value of the difference between predicted and observed transport rates. Accuracy does not vary with sample size for the predictive approach, because transport samples are not used. For purposes of illustration, accuracy for the predictive approach is assigned a value of 0.5 in Figure 1b. Accuracy for the empirical approach may be assumed to increase with the square root of the number of samples (e.g., the accuracy of predicting a mean

varies with $\sigma/(N)^{0.5}$, where σ is the sample standard deviation and N is the number of samples). The value of ε asymptotically approaches zero as N increases, so the accuracy for the empirical approach approaches one at large N. For the combined case, the accuracy with no samples is equal to that of the predictive approach. The increase in accuracy is again assumed to increase with the square root of N, approaching one at large N.

One way to examine the tradeoff between accuracy and cost is to examine their ratio, which gives a measure of value so that larger values imply more accuracy per cost (Figure 1c). For the predictive case, accuracy does not vary with sample size, so the accuracy/cost ratio is a constant. For the empirical approach, the accuracy/cost ratio first increases, then reaches a maximum and decreases with further N, as should be expected when cost increases linearly with N, whereas accuracy increases with its square root. This suggests that a maximum "value" of accuracy is obtained at an intermediate value of N (N=12 for the case illustrated). For the combined case, a maximum value of the accuracy/cost ratio also occurs, but at a smaller sample size (N=6). Thus, fewer samples are required to reach the maximum accuracy/cost value, and this maximum occurs at a larger value of accuracy for the combined (0.80) vs. the empirical (0.69) case.

The relative magnitude of some of the trends in Figure 1 will change if a different but equally reasonable set of parameter values are chosen. For example, the relative advantage of the predictive and empirical approaches depend entirely on the value of accuracy assigned to the predictive approach and the sample standard deviation assigned to the empirical transport samples. Some of the other results, however, may be quite general because of reasonable constraints that exist for some of the assumptions. In particular, if the accuracy of the combined approach can be assumed to be at least as large as that of the predictive approach, and if the accuracy in both the empirical and combined approaches increases with the square root of sample size, then the accuracy and accuracy/cost ratio for the combined approach should exceed those of either of the other two and a maximum value of the accuracy/cost ratio, should it exist, will occur at a smaller N for the combined approach. Of course, the actual existence of this solution and its practical utility depend on defining a method that effectively uses a small number of transport observations to increase the accuracy of the transport predicted by a model. A possible combined method is described later in this report, after the two-fraction transport model has been presented.

Physical Basis

Relative Mobility of Sand and Gravel

For the case of narrowly-sorted sediment, the influence of grain size on transport rate is well known empirically and may also be deduced from elementary physical considerations. The fluid force F_f acting on a grain may be represented by the fluid shear stress (force per area) τ_0 acting on the bed, multiplied by the exposed area of the grain, which is proportional to the square of the grain diameter D, or $F_f \propto \tau_0 D^2$. The resistance to motion may be assumed to be proportional to the submerged grain weight $F_g \propto (\rho_s - \rho)gD^3$, where ρ_s and ρ are the density of the sediment and water, respectively, and g is gravity. The ratio of the disturbing and resisting forces, known as the Shields parameter,

$$\tau^* = \frac{\tau_0}{(\rho_s - \rho)\, gD} \qquad (1)$$

has been found to effectively represent the combined effect of flow strength and grain size. An important indicator of this is that the transport rates of narrowly sorted sediments of different grain sizes may be made to collapse to a single curve when the flow is represented by τ^*. Values of τ^* are generally quite small, on the order of 1/20 for conditions near the onset of grain motion.

When grains of different size are mixed together, an additional grain size effect is important, the size of a grain *relative* to the remainder of the mixture. Smaller grains will tend to be hidden from the flow and their motion will be impeded by the presence of coarser grains on the bed, a process commonly known as "hiding". Larger grains will tend to be more exposed to the flow and their motion will be relatively easier compared to that possible over a bed of comparably sized grains. These relative size effects tend to counter the absolute size effects represented in τ^*. The extent of this balancing depends on a number of factors, including the spread of the bed size distribution, the proportion of fines, and the degree to which grains of different sizes are locally sorted on the bed.

In a gravel bed with a small amount of sand (less than approximately 10%), the absolute and relative size effects nearly balance, so that all sizes move at about the same rate at a given flow (when the transport rates are scaled by the proportion of each fraction in the bed). When a larger amount of fine material is present in the bed, the sand will tend to begin moving at smaller flows

than the gravel, and will move at greater rates at the same flow. There are several reasons for this. As the pore space among the coarser grains becomes increasingly filled, more of the sand remains close enough to the surface and is subject to entrainment and transport even when the gravel does not move. The sand can also collect into relatively well-sorted patches or streaks (Iseya and Ikeda, 1987; Ferguson et al, 1989; Wilcock, 1993; Paola and Seal. 1995), thereby eliminating most of the hiding effects on the small grains and allowing the absolute size advantage to dominate.

Framework and Matrix

An important principle guiding development of a two-fraction sediment transport model is the distinction between the finer (matrix) and coarser (framework) grains within the bed. In gravel-bed rivers with less than 20-30% sand, the bed is composed of a framework of gravel and cobbles with finer sediments filling the pores of this structure. This is termed a clast-supported bed. As the amount of sand increases, more of the framework grains are no longer in direct contact with each other and instead rest on matrix grains. Over the range in sand content of approximately 30% to 50%, the number of clast-clast contacts decreases to nearly zero and the bed is termed matrix supported.

Framework grains may be interlocked or imbricated, which increases their resistance to motion. Some framework grains on the surface bed surface may be relatively easy to move, while the motion of others may require entrainment of adjacent grains. At a given flow, some gravel grains exposed on the bed surface may remain immobile over the course of the flow, while others are occasionally entrained. This is called a state of partial transport (Wilcock and McArdell, 1993, 1997). As flow strength increases, the rate of motion of active grains will increase and the proportion of grains that are active may also increase. Thus, the gravel transport rate will increase very rapidly over the generally narrow range of flow required to break up the gravel framework. Large gravel transport rates require disruption of the bed structure.

In contrast, significant sand transport can occur without disturbance of the overall bed framework, as long as some sand is exposed to the flow. This requires enough fines content that the pore spaces between the framework grains are at least partially filled.

Influence of Fines Content on Sand and Gravel Transport

The behavior of the sand and gravel portions of the bed will vary as the proportion of sand increases. This is related to a number of factors, including the exposure the sand grains, the ability

of sand to become sorted into relatively homogeneous patches, and the transition from a framework-supported to a matrix-supported bed. Here, a qualitative description is given of the influence of fines content on the transport of both the sand and gravel fractions. The purpose is to provide a conceptual basis and some physical intuition for some of the trends that are evident in the transport data and for the choices made in reducing that data to a relatively simple model. The conceptual model is distilled from a wide range of observations by the author and others (e.g. Parker and Klingeman, 1982; Jackson and Beschta, 1982; Diplas and Parker, 1985; Beschta, 1987; Ferguson, Ashworth and Prestegaard, 1989; Wilcock and Southard, 1989; Wilcock, 1993; Wilcock and McArdell, 1993, 1997; Paola and Seal, 1995; Wilcock, 1997)

When the sand content in the bed is small (less than roughly 10%), the sand tends to be well hidden among the gravel clasts. If the size of the sand grains is small enough, most grains can settle through the bed surface layer, making them unavailable for further transport until the surface gravel clasts are entrained. There is not sufficient sand in transport to make persistent patches. Substantial sand transport requires disruption of the gravel framework, so that the sand and gravel tend to begin moving at any substantial rate at comparable flows. Further, the rate at which transport increases with flow strength is similar for the fine and coarse grains because the entrainment of coarse grains is necessary to make additional sand available for transport.

At larger sand contents (on the order of 10% to 30%), the bed is still clast-supported, but the pore spaces are relatively filled with sand. This leaves sand available for transport, even at flows too small to move the gravel, so that active sand transport may proceed without disturbing the bed framework. Furthermore, moving sand may congregate into patches on the bed surface, further increasing their relative ease of transport. The combined effect of pore filling and patch formation is that measurable amounts of sand transport begin at lower flows and that sand transport will persist as long as there is an upstream supply.

The effect of the increased sand content on the gravel transport is more complex. Gravel mobility may be decreased as the pore space between grains is filled with sand. The gravel may also be partially or temporarily buried by sand, which will suppress the gravel transport rates. Once a gravel grain is entrained, however, it may move faster and further on the relatively smooth bed provided by the filled pores. It will also have a more difficult time finding a place to stop. The rate at which transport rate increases with flow strength is likely to be larger for the gravel than the sand for conditions of partial transport. This occurs because an increase in gravel transport rate

results from both an increase in the proportion of actively transported grains, as well as an increase in velocity and distance of grain movement each time a grain is entrained.

As fines content increases further, more of the gravel grains are no longer in contact with each other with the number of contacts approaching zero as the fines content exceeds approximately 50%. The bed is then matrix supported. Patch development should be extensive and sand transport rates should be similar to those for a bed of uniform sand. Gravel transport will commence at smaller flows than those producing transport of unisize gravel, because the gravel clasts can be entrained by removal and undercutting of the surrounding sand and, once in motion, the gravel will able to keep moving over the relatively smooth sand bed.

The influence of sand content on transport may be summarized (sand% is approximate):

Sand content <10%: Sand and gravel begin moving at similar flows. The flow magnitude corresponds to that necessary to entrain unisize gravel. At a given flow, sand and gravel transport rates are of comparable magnitude, if transport rate is scaled by the proportion of each fraction in the bed.

Sand content 10-30%: Sand fills the pores between framework grains and collects into well-sorted patches. The sand begins moving at a smaller flow the gravel and, for a given flow, is transported at a larger rate.

Sand content 30-50%: Transition from a clast-supported to a matrix-supported bed. Sand patches are extensive, causing the sand transport to become similar to that for a unisize sand. Active sand transport destabilizes gravel, decreasing the flow needed to initiate gravel motion.

Sand content >50%: Matrix-supported bed. Sand transport is comparable to that of a unisize sand bed. Sand motion causes gravel transport to occur at a flow much smaller than that needed to initiate motion of a unisize gravel.

For stream beds with more than about 10% fines, the combined effect of these processes is that the size of sediment in transport typically increases with flow strength. Over a range of flows with measurable transport, the transport rates of the coarser size fractions are often orders of magnitude smaller than those of the finer fractions, and the size distribution of the transported sediment has a smaller mean and variance than that of the bed [e.g. *Jackson and Beschta*, 1982; *Carling*, 1988; *Church et al.*, 1991; *Kuhnle*, 1992; *Wilcock and McArdell*, 1993; *Lisle*, 1995]. As

flow increases, the transported load coarsens and its size distribution approaches that of the bed [e.g. *Parker and Klingeman*, 1982; *Wilcock*, 1992].

Because discharge duration decreases with magnitude, flows producing finer-grained transport have longer duration and, in streams with widely sorted bed material, can produce much of the annual sediment load, which can be considerably finer grained than the river bed material (*Leopold*, 1992). A particularly striking example of this is provided by Coon Creek, in the Medicine Bow National Forest, Wyoming (Wilcox et al., 1996). There, the annual sediment load is trapped in a weir pond, is considerably finer grained than the upstream sediment bed (Figure 2). This emphasizes the importance of a transport model that can predict sand and gravel transport separately. Clearly, a transport model based on a characteristic grain size (e.g. D_{50}) could not predict the annual load on Coon Creek.

A striking demonstration of the interaction of sand content and transport was made in a series of eight flume runs by Ikeda and Iseya (1988). Sediment was fed into the flume at the same rate in each run. The sediment was composed of two sizes: well-sorted medium sand (0.35 mm) and fine gravel (2.7 mm). The proportion of each size was varied from run to run. At equilibrium, the sediment discharge from the flume must equal the input, so the total transport rate was essentially constant from run to run. Water discharge and water depth were also held nearly constant, so only slope (and, therefore τ_0) varied from run to run as the proportion of different sizes changed. In two runs, the sand feed was 0% and 20% of the total feed rate, and the relation between transport and τ_0 was the same as that for clean gravel. For runs with a sediment feed composed of 54%, 67%, and 100% sand, the transport-τ_0 relation was the same as that for sand only. Runs with a sand content in the feed of 30%, 41%, and 40% were transitional between the clean sand and gravel transport relations (Figure 3). These results suggest that a transition from clean gravel to mixture transport behavior occurs at a sand content between 20% and 30% and that the transition from mixture to clean sand transport behavior occurs at a sand content between 40% and 54%. Because these runs were conducted at only a single total transport rate, it is not possible to deduce the form of the sand or gravel transport functions. It is interesting to note that the difference in size between the two fractions is a factor of 8, which is not exceptionally large, and that both fractions are small compared to typical gravel-bed rivers.

Data Used

Although many aspects of the two-fraction transport model may be deduced from general observations of mixed-size sediment transport, the basic form of the model must be determined from transport data. Therefore, high quality transport data are needed to define it. It will also be advantageous if the data used represent a range of sediment and channel properties that is typical of gravel-bed rivers. The reported transport rates must be of good accuracy, which generally means that the transport samples must include all the transported load, or that a very large number of individual transport measurements were made. The size distribution of the transport must also be measured in order to determine the transport rates of different sizes. The observations should cover a range of transport rates, including conditions near the initiation of motion. The bed and transport must also have a range of sizes that is representative of a gravel-bed river; this requirement excludes many laboratory experiments. The flow measurements accompanying the transport observations must be sufficiently accurate to permit calculation of the mean flow velocity U and the bed shear stress τ_0.

These restrictions limit the number of available data to a relatively small set. Data from four field sites are used: Oak Creek, Oregon (Milhous, 1973), East Fork River, Wyoming (Emmett, 1980; Emmett et al., 1980 and 1985), Jacoby Creek, California (Lisle, 1989), and Goodwin Creek, Mississippi (Kuhnle, 1992). In two cases, Oak Creek and East Fork River, bed load was sampled in a slot extending across the entire river, providing an unusually complete record of sediment transport. On Goodwin Creek, only a portion of the total bed-load was sampled using a hand-held sampler, but the sampling was conducted in a concrete supercritical flow flume which funneled all of the transport into a narrow area in the center of the flume so that an unusually comprehensive measurement of the bed load was made. In Jacoby Creek, bed load was measured with a large number of Helley-Smith samples, providing an relatively complete data set for a typical field case, although the accuracy of the reported transport rates may be lass than for the other three cases. Although the data examined here are among the best available, none of the data sets are without problems, as will be discussed below for each of the cases. In addition to the field cases, data is used from one laboratory study of mixed-size transport (Wilcock and McArdell, 1993).

Details regarding each of these studies may be found in the original references. The nature of the streams, sediment, and sampling are only summarized here. Table 1 summarizes the

hydraulic and sediment characteristics of each case, along with the flow and transport measurements. Figures 4 and 5 present the grain-size distributions of the five sediments. Oak and Jacoby Creeks are coarse gravel-bed rivers with a small, but nonnegligible sand content. Goodwin Creek and the East Fork River are slightly larger and have a larger sand content. The laboratory sediment has a sand content similar to Goodwin Creek. A broad range of sand content (10-59%) is covered by the five cases.

Oak Creek is a small gravel-bed river in the Coast Range of Oregon (Milhous, 1973). Drainage area at the sample site is 6.7 km^2. Stream gradient near the sample site is 1.4%, with a bankfull width of approximately 6 m and a winter rainfall hydrograph. The median size of the bed material is 20 mm, D_{90} is 65 mm, and there is about 12% finer than 2 mm.

The Oak Creek data were collected using a vortex sampler spanning the channel width (Milhous, 1973). Although the Oak Creek transport observations appear to be of exceptionally high quality for the gravel fractions, the vortex trap and sampling arrangement was evidently not efficient in trapping the finer fractions. The efficiency of the vortex trap is evident from the observation of sand collected in a second, unused, trap immediately downstream of the vortex slot (Milhous, 1973). Milhous also explains that a portion of the sand caught in the vortex trap would be lost from the sampling box at the trap exit. Because there are two sources of sand loss from the sampling system, it is difficult to estimate the magnitude of this loss. The data are presented without any adjustment for sand loss and their analysis must be made with these losses in mind.

The Oak Creek data are of interest for several reasons. First, it has been observed that all size fractions in the Oak Creek bed begin moving at nearly the same shear stress (Parker et al., 1982), a condition that would suggest that little selective transport of fine sediment occurs. Second, these data have been the subject of considerable debate, much of it arising from the incipient motion observations, so that the Oak Creek data have become quite familiar to many in the sediment transport community and provide the closest thing we might have to a standard.

Jacoby Creek is a single thread gravel-bed river in the Coast Range of Northern California (Lisle, 1986, 1989). Drainage area at the sample site is 36.3 km^2. Stream gradient near the sample site is 0.6%, with a bankfull width of 17.6 m, bankfull discharge of 19.6 m^3/s and a winter rainfall hydrograph. The median size of the bed material is 20 mm, D_{90} is 88 mm, and there is about 10% finer than 2 mm. Transport rates were sampled with a three-inch Helley-Smith sampler. Because of the size of the sampler opening, transport rates are reported only for sizes

finer than 32mm. Because 37.4% of the bed (based on a subsurface size distribution) is coarser than 32 mm, the actual transport of gravel is larger than that reported.

Goodwin Creek is a single thread gravel-bed river within a monitored drainage basin in north-central Mississippi (Kuhnle, 1992). Drainage area at the sample site is 17.9 km^2. Stream gradient near the sample site is 0.3% and bankfull width is 25 m. Transport occurs during intense convective rainfall events. The median size of the bed material is 8.3 mm, D_{90} is 30 mm, and there is about 34% finer than 2 mm.

Transport sampling was conducted in a "V"-shaped concrete supercritical flow section that captured all of the flow and transport (Kuhnle, 1992). Sampling was done with a Helley-Smith sampler modified to fit snugly on the bottom of the sampling section and which apparently trapped grains of all sizes with equal efficiency.

Although the transport data for Goodwin Creek are of exceptionally high quality, there is some uncertainty in the calculated bed shear stress. The apparent hydraulic roughness of the channel is much greater than would be expected for the grain size of the bed, suggesting that a sizable proportion of the total stress is form drag. Values of observed hydraulic roughness ($n \approx 0.06$; Bowie, 1989) are large relative to that which might be expected for a clean, straight channel with $D_{90} \approx 30$mm and $D_{max} \approx 64$ mm, for which values of n on the order of 0.02 to 0.03 might be expected (Henderson, 1969). Back-calculated values of the equivalent grain roughness k_s are on the order of 1 m to 2 m in the flow resistance formula

$$\frac{U}{\sqrt{gRS}} = 2.5 \ln\left(\frac{11R}{k_s}\right)$$

where U is mean velocity, S is water surface slope, R is hydraulic radius, and g is the acceleration of gravity. Part of the apparent form drag is presumably due to large gravel dunes that can develop in the test section upstream (Kuhnle and Bowie, 1994). Thus, it is likely that the total range of shear stress acting on the grains may be narrower than that given by the depth-slope product, although the actual values of skin friction remain uncertain. As a result, more emphasis in this discussion is placed on the high quality transport rate and size distribution information and the variation of transport with τ_0 must be treated with caution.

The East Fork River is a single thread sand and gravel-bed river in the Wind River Range of Wyoming (Emmett, 1980; Leopold and Emmett, in prep.). Drainage area at the sample site is

466 km^2. Stream gradient near the sample site is 0.07%, with a bankfull width of 19 m, bankfull discharge of 20 m^3/s and a snowmelt hydrograph. The median size of the bed material is 1.2 mm, D_{90} is 28 mm, and there is about 59% finer than 2 mm. The size distribution of the East Fork may be interpreted as that of a gravel-bed river with a median size of perhaps 16mm, to which a large amount of sand and pea gravel has been added. The source of this added sediment is Muddy Creek, a tributary to the East Fork River. Irrigation return flow diverted from the East Fork has increased the sediment supplied from Muddy Creek (Leopold and Emmett, in prep.).

Transport rates were sampled in a slot extending the full width of the channel. A conveyor belt inside the slot carried the trapped bed load to the bank, where it was sampled (Emmett, 1980; Leopold and Emmett, in prep.). A total of 132 transport samples were taken between 1973 and 1979; 118 of these samples are used here. The 13 excluded samples were all among the first few samples taken each year, all of which had exceptionally large transport rates and contained essentially no gravel.

The field observations are supplemented by laboratory flume data (Wilcock and McArdell, 1993). These data are for a sediment, the Bed of Many Colors, BOMC, that is unusual in two regards. First, the range in grain sizes (0.21 mm to 64 mm) is unusually wide for experiments involving recirculation of the load, but is representative of many gravel bed rivers and, by chance, very similar to the size distribution of Goodwin Creek (Figure 4). Second, the entire sediment was sieved into 14 1/2ϕ fractions and each fraction was painted a different color, permitting ready identification of individual fractions (and, in many cases, individual grains) on the bed surface. These observations include the proportion of grains of each size remaining immobile on the bed surface over the course of a run, a particularly useful observation for the purpose of evaluating the extent of mobilization of the bed surface. The wide range of grain size, together with the greater control and accuracy possible in the lab. make these data a useful addition to the transport observations used here.

Both sediment feed and sediment recirculating runs have been conducted with BOMC; the runs discussed here are for a recirculated sediment load. These runs are appropriate for the case considered here, the prediction of transport rate from the characteristics of the bed. In a recirculating flume, the transport rates depend directly on the flow strength and bed composition.

Grouping of Data

Variability in transport rate observations can arise from either sampling error (sampled rate does not equal the actual transport rate through the section) or natural variability (spatial or temporal). To reduce the influence of this variability on the empirical relations to be developed, the transport samples for similar flows were grouped for each case. Grouping involves a tradeoff between larger groups (providing more stable averages) and a small range in flow (so that transport rates for similar flow conditions are combined).

For the East Fork River, 118 samples were combined into 18 groups (Figure 6). The samples were grouped by discharge, which was presumed to be the most accurately measured flow variable. The ratio of largest to smallest discharge within each group is less than 1.1, except for the smallest discharge (Q=3.84), where the data is more sparse and the ratio is 1.22. All groups contain at least four samples, except for a sample of two at Q=5.55 cms, where the data is sparse, and the single largest Q' (41.5 cms), which is 30% larger than the next largest Q'. Within each group, hydraulic and transport measurements were combined using geometric averages.

For Oak Creek, the winter 1971 data are used, which Milhous (1973) reports are the highest quality data available. The transport data for the 34 largest discharges ($Q > 0.5$ m^3/s) are combined into nine observations by grouping samples with similar transport rates.

For Jacoby Creek, 105 samples were combined into 15 groups (Figure 7). The largest grouped sample was for overbank flow and is not included in the analysis. The maximum discharge for samples used is 18.5 m^3/s (bankfull discharge is 19.6 m^3/s). The smallest three grouped samples deviate somewhat from main trend and were also dropped from the analysis. Based on a reported maximum sample duration of 120 s, the typical sample size for these smaller transport rates would be smaller than 5 g, suggesting that sample error with the Helley-Smith sampler may have been large. For the 11 groups used, the smallest number of combined samples is five and the ratio of largest to smallest discharge within each group is less than is 1.20 (7 are less than 1.10, 3 are between 1.13 and 1.20).

The transport samples for Goodwin Creek were grouped by Kuhnle (1992). The results of 488 transport observations were combined into six groups within τ_0 ranges of 5 Pa. Transport samples for the Bed of Many Colors were grouped by Wilcock and McArdell (1993). For each of

the eight runs examined here, transport observations were made until a steady mean value could be determined.

Boundary Between Sand and Gravel

In order to develop a two-fraction transport model, a boundary between sand and gravel sizes must be defined. The boundary could be specified as a particular grain size or as the size corresponding to a specified proportion of the bed sediment size distribution. The choice made here is to define the sand/gravel boundary as D = 2mm, the conventional boundary between sand and gravel in most size scales. An exception is Oak Creek, for which the sand/gravel boundary is 2.38 mm, because no 2mm sieve was used in the size analysis (Milhous, 1973).

A fixed grain size boundary is simple and consistent and permits a direct investigation of the effect on transport of changes in fines content. In contrast, defining the fines content as a fixed percentage of the bed material eliminates the possibility of investigating the influence of changes in fines content. It also eliminates the use of narrowly sorted sediment as an obvious end member in describing the behavior of sand and gravel as a function of sand content.

For coarse, narrowly sorted sediment, the grain size associated with a fixed percentage could be much larger than that commonly associated with fines or sand. Further, the addition of fine sediment to a channel would cause the sand/gravel boundary to shift, which is likely to cause confusion in interpreting and presenting the results. Some environmental concerns (e.g. spawning success, invertebrate habitat; intrabed flow) depend more directly on the actual size of matrix material, rather than the proportion of material finer than a fixed percentage.

The representative size of the sand and gravel fractions is taken to be the median of each fraction. That is, the sand size D_s is the median for all grains finer than 2 mm and the gravel size D_g is the median for all grains coarser than 2 mm.

Model Development

The transport rates of sand q_s and gravel q_g are expressed in units of sediment mass transported per unit width and time. In the model, q_s and q_g are taken to depend on three general variables

(1) the size of each fraction, represented by its median size (D_s and D_g),

(2) the amount of each fraction in the bed (f_s and f_g),

(3) the flow strength, measured by the magnitude of the bed shear stress τ_0 relative to the value of τ_0 at which motion begins, known as the critical shear stress (τ_{cs} and τ_{cg}).

In a general form, the transport relations considered are

$$q_s = f_s f_s(D_s, \tau_0, \tau_{cs}, \rho, \rho_s, g) \quad (2a)$$

$$q_g = f_g f_g(D_g, \tau_0, \tau_{cg}, \rho, \rho_s, g) \quad (2b)$$

where f_s and f_g are the transport relations, or functions, to be developed here. Fluid density ρ, sediment density ρ_s, and the acceleration of gravity g influence the transport directly by determining the submerged grain weight and influence the transport indirectly through their effect on the turbulent dynamics of the flow and the nature of waves on the water surface. These variables are included in Eq. 2 for completeness, but are not directly considered in this work, which focuses only on quartz-density sediment in water under conditions of subcritical flow.

The total bed-material transport rate q_b is $q_b = q_s + q_g$, and $f_s + f_g = 1$.

Even though Eq. 2 appears quite general, several important assumptions have been made. First, it is assumed that the transport functions f_s and f_g are independent of f_s and f_g. That is, although the calculated transport rate will depend directly on f_s and f_g, as shown in Eq. 2, the form of f_s and f_g are assumed to not vary with sand content. The functions f_s and f_g represent the transport capacity for sand and gravel, which is the transport rate that would occur if the bed were entirely composed of either sand or gravel ($f_g = 1$ or $f_s = 1$). When transport data are compared to possible general transport relations, the transport rates are plotted as q_s/f_s and q_g/f_g, which, by Eq. 2, should equal f_s and f_g, respectively.

The second assumption is that other variables representing the flow, such as depth, velocity, and slope are not explicitly included. It is assumed that their influence on q_b is accurately represented by τ_0.

The third assumption is that the transport functions for each fraction are assumed to depend on the grain size of that fraction, but not the grain size of the other fraction. This is why D_s (but not D_g) appears in Eq. 2a and *vice-versa* for Eq. 2b. That is, q_s and q_g are assumed to depend on D_s and D_g, respectively, but not on the ratio D_s/D_g. In essence, this assumption, together with the role of f_s and f_g considered above, mean that a unique transport function is defined for each fraction and that this function will not vary with either the proportion of that fraction on the bed or with the grain size of the other fraction. If this assumption is incorrect, trends in the observed q_s and q_g will be found to vary with either sand content or the relative size of sand and gravel.

Finally, no characteristics of the bed size distribution other than the median size of each fraction are included in Eq. 2. Other size parameters, such as the standard deviation of the size distribution or some measure of the bimodality or skew of the distribution, might be included. It is assumed that, if the bed sediment is divided into two separate populations, the resulting size fractions will have simple unimodal distributions, for which the influence of other size parameters has been shown to have little influence on the transport of individual fractions within the mixture (Wilcock, 1992; 1993).

Dimensional analysis may be used to reduce the list of eight variables in each of Eq. 2a and 2b to a list of five nondimensional groups without any loss of generality. There are numerous valid versions of such a list; one that is useful for the present purposes is

$$\frac{q_{bi}}{\rho_s \sqrt{(s-1)\, g\, D_i^3}} = f\left(f_i,\ s,\ \frac{\tau_0}{(s-1)\rho g D_i},\ \frac{\tau_{ci}}{(s-1)\rho g D_i} \right) \tag{3}$$

where $s = \rho_s/\rho$, and the subscript i represents either sand or gravel. The dimensionless transport rate is often referred to as the Einstein transport parameter q^*

$$q^* = \frac{q_b}{\rho_s \sqrt{(s-1) g D^3}} \tag{4}$$

The dimensionless shear stress is generally referred to as the Shields parameter τ^*

$$\tau^* = \frac{\tau_0}{(s-1)\,\rho g D} \tag{5}$$

Using these definitions, Eq. 3 may be expressed more compactly as

$$q_i^* = f\,(f_i,\ s,\ \tau^*_i,\ \tau^*_{ci}) \tag{6}$$

An alternative dimensionless transport rate can be defined by dividing q^* by $(\tau^*)^{1.5}$

$$W^* = \frac{q^*}{(\tau^*)^{1.5}} = \frac{(s-1)\,g\,q_b}{(\tau_0/\rho)^{1.5}} \tag{7}$$

If τ^* is retained as a separate variable in Eq. 6, there is no loss of generality if q^* is replaced by W^*. It is commonly observed that q^* becomes proportional to $(\tau^*)^{1.5}$ at large τ^*, so that W^* approaches a constant in the limit of large transport rates. The most important advantage of W*, however, is that it does not contain grain size, allowing a single transport function to be defined for all grain sizes, should one exist.

If it is argued that τ_{ci} influences transport rates only as a reference value of τ_0, τ^*_{ci} may be divided into τ^*_i in Eq. 6 and dropped from the list. If we further restrict our attention to quartz density sediment in water, ρ_s/ρ is a constant (s = 2.65) and need no longer be included. Dividing τ^* by τ^*_c, dropping τ^*_c and s from the list, and replacing q^* with W*, the list of dimensionless variables becomes

$$W_i^* = f\left(f_i,\ \frac{\tau_0}{\tau_{ci}}\right) \tag{8}$$

Put in the form of Eq. 2, this is for each fraction

$$\frac{W_s^*}{f_s} = f_s\left(\frac{\tau_0}{\tau_{cs}}\right) \tag{9a}$$

$$\frac{W_g^*}{f_g} = f_g\left(\frac{\tau_0}{\tau_{cg}}\right) \tag{9b}$$

where f_s and f_g have been removed from the transport function, consistent with the assumption that f_s and f_g are independent of sand content. Comparison of Eq. 2 and Eq. 9 shows that grain size is included in Eq. 2, but is no longer explicitly present in Eq. 9. This results from replacing q^* with W^* and, more importantly, replacing the two dimensionless variables τ^*_i and τ^*_{ci} in Eq. 6 with the single dimensionless group τ_0/τ_{ci}. The influence of grain size remains in Eq. 9 in two ways. First, τ_{ci} depends directly on grain size so that, for a given flow, τ_0/τ_{ci} will vary with grain size. Second, separate transport functions f_s and f_g are defined for the sand and gravel, so that the form of the transport function may vary with grain size.

The absence of any explicit reference to grain size in Eq. 9 neatly summarizes two of the important assumptions that have been made. First, it is assumed that the transport rates of the sand will depend on D_s (through its influence on τ_{cs}), but will not depend the gravel grain size D_g. Similarly, the transport rates of the gravel will depend on D_g (through its influence on τ_{cg}), but will not depend the sand grain size D_s. The second assumption is that the scaled transport rates W^*_i/f_i depend only on the amount by which τ_0 exceeds τ_{ci} (that is, on the excess shear τ_0/τ_{ci}) and will not depend explicitly on the grain size of either the sand or gravel. The result is that two unique transport relations are hypothesized—one for sand and the other for gravel—and these transport functions are taken to hold for any grain size and any sand content. The test of this hypothesis and its supporting assumptions comes in the attempt to collapse the transport data to two transport functions. If the hypothesis is not correct, it will not be possible to find a common transport function in the form of Eq. 9 when the actual transport data are considered.

For a general predictive model, both the transport functions f_i and the critical shear stresses τ_{ci} must be determined. A separate means, then, is needed for predicting τ_{ci}. That is, four predictive functions are sought, one each for f_s, f_g, τ_{cs}, and τ_{cg}. In this work, two options for predicting transport are presented. The first is a completely predictive one, in which f_s, f_g, τ_{cs}, and τ_{cg} are predicted as a function of the bed sediment and channel properties. In the second, the flow producing incipient motion is measured in the field, so that a predictive relation for τ_{cs} and τ_{cg} is not needed. As will be discussed later, the latter approach is preferable because there is considerable uncertainty in estimating the discharge that produces τ_{ci} and much of this uncertainty can be removed if this discharge is determined by direct observation. Even in the case of directly measured τ_{ci}, however, demonstration that τ_{ci} can be consistently predicted in a fashion consistent

with the physical processes already described lends general support to the transport functions developed and to the hypothesis that unique and consistent transport functions exist.

Calculation of Bed Shear Stress

Part of the total force exerted by the river on its bed and banks acts on the bed sediment, producing sediment transport. The remainder of the flow force acts on channel banks and any objects in the flow and does not produce sediment transport. In analyzing or predicting sediment transport rates, the objective is to determine that portion of the total boundary shear stress τ_0 that is effective in producing sediment transport. Because the effective shear stress τ' (sometimes called the skin friction) is only a portion of the total boundary shear stress, the method is often called drag-partitioning.

The method used here to estimate τ' is based on that of Einstein (1950), although the presentation is somewhat different. A number of more sophisticated drag-partitioning methods have been proposed in recent years (e.g. Wiberg and Smith, 1991; Nelson et al., 1991). Although the physical basis for these methods is more complete, the data and computational requirements are also more extensive than those associated with the Einstein method. The Einstein approach has been found to give stable estimates of τ' that correlate well with observed transport rates (the true value of τ' cannot be measured directly, so indirect confirmation of a method's reliability depends on its physical plausibility and the strength of its correlation with observed transport). As will be discussed below, when the recommended approach for calculating transport rates is followed, the transport rates depend primarily on the ratio of τ' to τ_{ci}, rather than on τ' directly, so some of the error in estimating τ' should cancel and any method that gives a consistent increase of τ' with Q should suffice.

In a uniform wide flow, the mean velocity U is related to the bed shear stress (represented by the shear velocity $u_* = (\tau_0/\rho)^{0.5}$), the flow depth h and the hydraulic roughness k_s of the bed sediment by the Keulegan logarithmic velocity profile

$$\frac{U}{u_*} = 2.5 \ln\left(\frac{11\,h}{k_s}\right) \tag{10}$$

For these flow conditions, $u_* = (ghS)^{0.5}$, so (10) becomes

$$\frac{U}{\sqrt{ghS}} = 2.5 \ln\left(\frac{11\,h}{k_s}\right) \tag{11}$$

Eq. 11 should hold for steady uniform flow in a wide channel for which the hydraulic roughness is provided entirely by the bed sediment. If some part of the flow force is expended on elements other than the bed grains (banks, bed forms, trees, boulders, etc.), the actual hydraulic roughness must be larger than k_s in order to correctly relate h and U. The assumption made by Einstein (1950; and later by Engelund, 1967) was that, when a part of the flow force is expended on elements other than the bed grains, Eq. 11 still approximately represents the skin friction τ' if h is no longer interpreted as the actual flow depth, but as that fraction of the flow depth that corresponds to the actual shear stress acting on the bed. That is, if all of the boundary shear stress acts on the bed grains, the hydraulic roughness is represented by k_s and h in Eq. 11 is the actual flow depth. If only part of the boundary shear stress acts on the bed grains, the depth calculated using the observed U and k_s in Eq. 11 will be smaller than the actual flow depth. This smaller "effective" depth (h') is used to calculate the effective shear velocity $u_*' = (gh'S)^{0.5}$. The effective shear stress τ' is given by $\tau' = \rho g h' S$.

The effective depth h' is calculated from Eq. 11 as

$$h' = \frac{1}{g\,S}\left[\frac{0.4\,U}{\ln\left(\frac{11\,h'}{k_s}\right)}\right]^2 \tag{12}$$

Because h' is found on both sides of Eq. 12, the solution is iterative, although it converges quickly.

Calculation of τ' requires selection of the roughness size k_s. For consistency, k_s in each case was chosen to be twice the D_{65} of the overall bed size distribution. This size has been found to give good results for both field and flume results (Engelund, 1967; Wilcock, 1993). In the remainder of the report, τ' will be used to represent the bed shear stress, and the prime notation is dropped.

The Data

Sand and gravel transport rates are presented as a function of skin friction shear stress in Figure 8. The data for Oak and Jacoby Creeks are separated from the other three cases, a result of

their larger grain size. The sand content of Oak and Jacoby Creeks is small and it is seen that, in both cases, the fractional transport rates for sand and gravel are similar. The sand and gravel sizes for Goodwin Creek, East Fork River, and BOMC are similar, and these transport data tend to cluster. In these cases, the sand content is much larger and the sand and gravel transport curves diverge. Sand begins moving at a smaller τ and the ratio q_s/q_g is large at small τ. As τ increases, this ratio decreases, approaching one at the largest transport rates measured.

Critical Shear Stress

Eq. 9 gives the basic structure of the transport function sought and the framework within which the transport data will be analyzed. The essential goal is to determine from the data whether unique functions f_s and f_g can be defined solely as a function of (τ/τ_{ci}). Before this can be done, values of τ_{cs} and τ_{cg} must be determined for each of the sediments investigated.

Because τ_{ci} is difficult to define or observe, it is often replaced by a reference shear stress τ_r, which is the value of τ_0 that produces the small reference transport rate $W^* = 0.002$. This is accomplished by plotting the transport data as a function of τ_0 and finding the value of τ_0 at which $(W_i^*/f_i) = 0.002$. This is a straightforward matter when the transport observations include values both larger and smaller than $(W_i^*/f_i) = 0.002$. In some cases, particularly with finer fractions, the smallest observed transport rate is larger than $(W_i^*/f_i) = 0.002$, so some extrapolation to the reference level is necessary. Extrapolation beyond a small fraction of an order of magnitude prevents an independent determination of τ_{ri}. In effect, the solution to the problem (the form of f_s and f_g) must be assumed in order to carry out the extrapolation.

A line representing $W^* = 0.002$ is plotted on Figure 8. For the units of that figure, the reference line is given by $q_{bi} = 0.01035\ \tau_0^{1.5}$. Values of τ_{ri} chosen for all ten fractions are shown as small symbols on the figure. Values of τ_{ri} for Oak and Jacoby Creeks and for BOMC are fitted by interpolation or short extrapolation. For Goodwin Creek and East Fork River, an independent fit of τ_{ri} is not possible, because the transport rates do not extend close enough to the reference line. In these cases, values of τ_{ri} were chosen to provide the best collapse of fractional transport rates (see following section). In these two cases, τ_{ri} is an outcome of the similarity collapse used to develop f_s and f_g, rather than directly measured from the data.

Values of τ_{ri} may be expected to depend on the grain size of the sand and gravel fractions and on the proportion of fines in the bed. The effect of absolute grain size is included in the

Shields parameter τ_{rs}^* and τ_{rg}^*. The variation of τ_{rs}^* and τ_{rg}^* with fines content is shown in Figure 9. Data are included not only for the five sediments considered here, but for an additional six laboratory sediments with purely bimodal size distributions (Wilcock, 1992, 1993; Kuhnle, 1993), which expand the range of fines content.

The values of τ_{rs}^* and τ_{rg}^* follow trends that are consistent with the well-established behavior of unisize sediments and the conceptual model of mixed-size transport discussed earlier in this report. Considering the gravel first, τ_{rg}^* approaches values of $\approx$0.04 when the sand content is small. This value is well established for clean, well-sorted gravels. The plotted value of τ_{rg}^* for Jacoby Creek is likely to be somewhat larger than the value that would correspond to the transport of all gravel coarser than 2mm. This is because transport rates are reported only for sizes finer than 32 mm (limited by the size of the sampler opening), whereas 37% of the bed sediment is coarser than 32mm. If q_g were doubled for Jacoby Creek, its value of τ_{rg}^* would fall closer to the value of 0.031 shown for Oak Creek. For large values of sand content, (>30%), τ_{rg}^* approaches an apparently constant value of $\approx$0.01. τ_{rg}^* decreases over the range of fines content 20-50% from a clean-gravel value of 0.03-0.04 to the sand-bed value of 0.01. The range over which this decrease occurs corresponds to the range of fines content separating relatively clean framework-supported gravel from a sandy, matrix-supported bed. That a minimum may exist for τ_{rg}^* is plausible. The influence on τ_{rg}^* of further increases in relative roughness (D_g/D_s) should be very small as D_g/D_s becomes very large, at which point τ_{rg} would be determined primarily by the grain mass.

The variation of τ_{rs}^* with sand content is similar to that for τ_{rg}^*. At large f_s, τ_{rs}^* approximately $\approx$0.04, the conventional value for narrowly sorted sediment. This small value of τ_{rs}^* persists until f_s decreases to less than approximately 0.4. For $0.2 < f_s < 0.4$, τ_{rs}^* increases rapidly with further decrease in f_s. The value of τ_{rs}^* for Oak Creek is probably smaller than that shown on Figure 9, because the true sand transport rate is larger than that measured. This would tend to make τ_{rs}^* for both Jacoby and Oak creek equal to about 0.5. This is probably not a general result, however. For small f_s, τ_{rs} should take a value close to τ_{rg} (which happens to be similar for Oak and Jacoby Creeks). Because τ_{rg} depends on the gravel size, which is not included in Figure 9.b, the plot of τ_{rs}^* at small f_s need not converge to a single value, even though its behavior is consistent and, therefore, predictable. Instead, $\tau_{rs}^* = \text{const.}\ \tau_{rg}^*\ (D_g/D_s)$, where const. = 0.8 is used in Figure 9b. That $\tau_{rs} \approx \tau_{rg}$ at small f_s results from the fact the available

sand tends to become hidden among the gravel pores. Significant sand transport requires entrainment of the gravel . The same relation is evident in Figure 8, where it is seen that $\tau_{rs} \approx \tau_{rg}$ for Jacoby and Oak Creeks. The decrease in τ_{rs}^* for $0.2 < f_s < 0.4$ occurs because the pore spaces begin to fill with sand and the sand forms segregated patches over this range.

Although the variation of τ_{rg}^* and τ_{rs}^* is apparently well described by sand content (and is also consistent with well known limiting values for clean sand and gravel), it is not likely that a high degree of accuracy in predicting transport rate may be achieved if values of τ_{ri} are chosen from Figure 9. Certainly this is the case for sand content between 20% and 40%, for which τ_{rg}^* and τ_{rs}^* vary rapidly, but there is little data to delineate the exact nature of this variation. However, even for other values of f_s, the transport rate predictions are likely to be inaccurate simply because transport rate varies so rapidly with τ/τ_r (note that the transport rates in Figure 8 span nearly seven orders of magnitude). Even a small error in estimating τ_{rg}^* and τ_{rs}^* will produce a large error in the calculated transport rate. This is the motivation for developing a hybrid approach (described later in this report) in which values of τ_{ri} are directly measured and then used directly in the prediction of transport rate.

Transport Function

The form of the transport functions f_s and f_g are to be determined from the transport data. The hypothesis is that the influence of grain size on fractional transport rates is entirely accounted for by its effect on the reference shear stresses τ_{rg} and τ_{rs}, so that unique functions of τ/τ_{ri} can be defined for the transport of sand and gravel. If τ_{ri} is accurately specified and a unique transport function exists for the sand and gravel fractions, all transport data for each fraction should collapse to a single relation between (W_i^*/f_i) and (τ/τ_{ci}). To test this hypothesis, a suitable dimensionless form is needed for examining the transport data. That the form given by Eq. 9 is correct is demonstrated on Figure 10, which shows the Parker-Einstein transport function (Parker, 1979; similar results would be achieved with other transport functions) plotted using W^*, q^*, and q_b for the transport and using τ/τ_c, τ^*, and τ for the shear stress. The transport function is plotted for three cases: D = 32mm with a critical shear stress of 21 Pa ($\tau^*_{cg} = 0.04$), D = 1mm with a critical shear stress of 21 Pa ($\tau^*_{cs} = 1.28$), and D = 1mm with a critical shear stress of 0.65 Pa ($\tau^*_{cs} = 0.04$). Note that in some panels on Figure 10, two or three of the relations fall directly on top of each other. The only combination that causes all three curves to collapse, regardless of

grain size and critical shear stress, is W^* *vs.* τ_0/τ_c. This, then, is the appropriate framework to use to look for a transport function that is independent of grain size and critical shear stress.

The analysis done here is not without precedent. Rather than defining an entirely new transport function, adding to an already long list, it is more appropriate to attempt to evaluate whether an existing transport function might work for the present purposes. A useful general function is

$$\frac{W_i^*}{f_i} = \alpha_i \left(1 - \frac{\tau_{ci}}{\tau_0}\right)^{\beta_i} \tag{13}$$

where α_i and β_i are a coefficient and exponent to be determined from the data. For $\beta_i > 1$, (W_i^*/f_i) increases rapidly at small values of (τ_0/τ_{ci}) and approaches a constant value at large values of (τ_0/τ_{ci}), as is commonly observed. With the appropriate choice of α_i and β_i, Eq. 13 represents several common transport functions, as shown in Table 2.

Model	α	β	ξ ($\tau_c = \xi\ \tau_r$)
Meyer-Peter and Müller (1948)	8.0	1.5	0.9960
Parker (1979)	11.2	4.5	0.8531
Yalin (1992)	4.5	1.0	0.9995

Table 2. Coefficient and Exponent for three transport functions.

The Parker formula is a power approximation of the Einstein (1950) bed-load curve. The Yalin formula is essentially that of Bagnold (1956).

When W_i^* in Eq. 13 is set equal to $W_r^* = 002$, $\tau_0 = \tau_r$ and Eq. 13 may be reduced to $\tau_c = \xi\ \tau_r$, where the value of ξ depends on the values of α and β. The values of ξ in Table 1 are slightly smaller than unity, indicating that τ_r is slightly larger than τ_c.

The sand and gravel transport rates are plotted as W_i^* *vs.* τ_0/τ_{ri} in Figure 11. In both cases, the consistency of the data collapse is remarkable. The Parker/Einstein transport function is superimposed on the gravel transport rates in Figure 11a. The degree of fit is very good. The

Parker/Einstein transport function does not provide a good fit to the sand transport, as shown on Figure 12, which is identical to Figure 11, except that both sand and gravel are shown on the same plot. The rate of increase of transport (the slope of the data) is greater for the gravel than for the sand. This may be expected because the increase in gravel transport for a given increase in τ_0/τ_{rg} will be produced by both an increase in grain velocity and by an increase in the proportion of grains in transport (Wilcock, 1997).

The other standard transport functions shown in Table 2 do not fit the sand transport rates (they are steeper, not gentler). An alternative function, chosen to be similar to the gravel function, is

$$\frac{W_i^*}{f_i} = \alpha_i \left(1 - \sqrt{\frac{\tau_{ci}}{\tau_0}}\right)^{\beta_i} \qquad (14)$$

Eq. 14 (labeled "Reduced Parker-Einstein") is shown on Figure 11b and Figure 12m using the same values of α_i and β_i as for the gravel relation. The fit is reasonably good, although some systematic deviation is evident, particularly in the Goodwin Creek data, which have a steeper trend than the other data (Figure 12). As explained earlier, there is uncertainty associated with estimated values of skin friction for Goodwin Creek because of the occasional presence of large gravel dunes in the channel (Kuhnle and Bowie, 1994). This uncertainty includes not only the magnitude of the estimated τ (which primarily influences τ_{rg} and τ_{rs}), but also the range of τ values (which influences the spread of τ/τ_{ri} values).

Model Application

Eq. 13 is the basis for predicting gravel transport rates, with $\alpha = 11.2$ and $\beta = 4.5$ (the Parker-Einstein transport model). Eq. 14 is the basis for predicting sand transport rates, with the same values of coefficient and exponent. These equations may be recast in terms of transport rate

$$q_g = \frac{11.2\,\rho_s\,f_g}{(s\text{-}1)g}\left(\frac{\tau_0}{\rho}\right)^{1.5}\left[1-\frac{\tau_{cg}}{\tau_0}\right]^{4.5} \tag{15a}$$

$$q_g = \frac{11.2\,\rho_s\,f_s}{(s\text{-}1)\,g}\left(\frac{\tau_0}{\rho}\right)^{1.5}\left[1-\sqrt{\frac{\tau_{cs}}{\tau_0}}\right]^{4.5} \tag{15b}$$

Using standard values for sediment and fluid density ($\rho_s = 2650$ kg m^{-3}, $\rho = 1000$ kg m^{-3}, $\rho_s/\rho = s = 2.65$), and gravity ($g = 9.81$ m s^{-2}), Eq. 15 becomes

$$q_g = 0.0580\,f_g\,\tau_0^{1.5}\left[1-\frac{\tau_{cg}}{\tau_0}\right]^{4.5} \tag{16a}$$

$$q_s = 0.0580\,f_s\,\tau_0^{1.5}\left[1-\sqrt{\frac{\tau_{cs}}{\tau_0}}\right]^{4.5} \tag{16b}$$

where q_g and q_s are in units of kg m^{-1} s^{-1} and τ_0, τ_{cg}, and τ_{cs} are in Pa (kg m^{-1} s^{-2}). Eq. 16 makes clear the input needed to calculate transport rate. One of f_s and f_g must be specified, the other is found from $f_s + f_g = 1$. Bed shear stress τ_0 must also be specified, along with values of the critical shear stress τ_{cg} and τ_{cs}. The value of τ_0 must be the skin friction, corresponding to the actual force per unit bed area producing bed material transport. The critical shear stresses may be either estimated from specified values of f_s, D_g and D_s, (using Figure 9) or they may be directly measured in the field. Both approaches are discussed here; the latter should give far more accurate results.

A remarkable feature of the similarity collapse leading to Eq. 16 is that D_s and D_g are not needed to estimate transport rate if τ_{rs} and τ_{rg} found from transport samples.

The necessary field observations include surveys of the channel profile and of the primary cross section (PXS), the bed surface grain-size distribution, and a rating curve (depth vs

discharge) at the PXS. Methods for obtaining all of these observations are clearly presented in Harrelson et al. (1994). Only observations that supplement this field manual are discussed here. If τ_{cg} and τ_{cs} are to be estimated, values of D_g and D_s for the bulk sediment bed are also needed. If τ_{cg} and τ_{cs} are to be found directly from the transport, observations are needed of transport rate in the vicinity of $W^* = 0.002$, the reference transport rate. These may be obtained with acceptable accuracy by installing sediment traps in the bed at the PXS.

Site Selection

The general objective is to determine the sand and gravel load passing through a stream section at a specified discharge. If the sediment load calculated or observed at a single cross section is assumed to represent the entire reach, it is implicitly assumed that the transport rate is uniform along the channel. Although this is not generally true in detail, if strongly nonuniform transport persisted over long periods of time, evidence of scour or deposition should be apparent. If transport observations are to be made, care should be taken to not locate the PXS downstream of likely sources of scour or deposition, such as recent channel disturbances, tight channel bends with large accumulations of fresh sediment, or large woody debris obstructing the flow and transport field.

The ideal PXS is in a straight channel reach with only modest variation in lateral bed topography. In a meandering reach, a section at the thalweg crossover is likely to give a more even lateral topography. The goal is to reduce lateral nonuniformity in transport, which should increase the accuracy of extrapolating transport observations at a few locations to the entire channel width. In addition to the channel geometry observations described by Harrelson et al. (1994), the width of active bed material transport must be estimated. In a gravel-bed river with steep vegetated banks, the active width should be relatively easy to identify. In other cases, it may be necessary to observe the extent of transport during bankfull flow.

Flow Calculation

The effective shear stress τ is estimated using the Einstein procedure described previously. Because the formula (Eq. 12) is iterative, it is convenient to replace it with

$$\frac{U}{u_*} = 8.1 \left(\frac{h}{k_s} \right)^{1/6} \tag{17}$$

which is nearly identical to Eq. 12 over most conditions relevant to this work. Using $u_* = (ghS)^{0.5}$, Eq. 17 may be shown to be the Manning flow resistance relation with the roughness n given by $n = 8.1\ g^{0.5}\ k_s^{1/6}$. Eq. 17 may be solved for h

$$h = \left(\frac{1}{g\,S}\right)^{3/4} \left(\frac{U}{8.1}\right)^{3/2} \left(k_s\right)^{1/4} \tag{18}$$

so that h can be found directly from specified values of S, U, and k_s. The value of h given by Eq. 18 should be smaller than the total flow depth. Using $\tau = \rho g h S$ and Eq. 18 to give h, the skin friction τ is given as

$$\tau = \rho \left(g\,S\,k_s\right)^{1/4} \left(\frac{U}{8.1}\right)^{3/2} \tag{19}$$

In application, the value of U is found from the section rating curve (Harrelson et al., 1994) and the relation between cross-sectional flow area and stage for the PXS. If the flow is approximately uniform over a channel length of more than 10 channel widths, the water surface slope may be used to calculate τ. Otherwise, it will be necessary to estimate the mean velocity at adjacent sections and use slope of the energy grade line ($EGL = z_s + U^2/2g$, where z_s is the water surface elevation). The roughness k_s may be calculated as $k_s = 2D_{65}$, where D_{65} is determined from a pebble count.

Using $k_s = 2D_{65}$ and conventional values of water density ($\rho = 1000\ kg\ m^{-3}$) and gravity ($g = 9.81\ m\ s^{-2}$), Eq. 19 becomes

$$\tau = 16.2 \left(S\,D_{65}\right)^{1/4} U^{3/2} \tag{20}$$

where τ is in Pa, D_{65} is in mm, and U is in m/s.

Several points are worth noting about the procedure given here for estimating skin friction τ. S and U are both measured quantities; D_{65} is also measured, but provides only an estimate of k_s. Because S and k_s are raised to the 1/4 power, however, the dependence of τ on these two variables is relatively weak. Of more importance is the error in the calculated transport produced by error in τ. Innacurate transport estimates arise both from error in estimating the section-average value of τ and from the fact the τ varies across the section. Because the transport rate is a strong

nonlinear function of τ, both sources of variability in τ can produce large errors in the calculated transport. In fact, this is the largest source of error in any transport estimate, whether based on the present method or not. This problem motivates the second option given here for predicting transport rates, in which τ_r is directly estimated from transport observations. In the region of the transport relation most sensitive to τ (as τ approaches τ_c), the calculated transport rate depends primarily on the ratio τ/τ_c, rather than the actual value of τ. The ratio τ/τ_c can be estimated with greater accuracy than either τ or τ_c individually because much of the error in estimating the bed shear stress may be expected to cancel when forming the ratio.

Sediment Observations

The hydraulic roughness k_s is based on D_{65} of the bed surface size distribution. D_{65} is determined from a pebble count within ±1 channel width of the PXS. If τ_{rs} and τ_{rg} are to be estimated, values of D_s and D_g must be found from bulk samples at the PXS. The size of the bulk sample should be sufficiently large that the single largest clast in the sample takes up no more than 2% of the total sample weight. If the sediment size varies across the section, multiple samples should be taken to provide a representative size distribution. Church et al., (1987) provide further guidance on sampling for size distribution.

A remarkable feature of the similarity collapse leading to Eq. 16 is that D_s and D_g are not needed to estimate transport rate if τ_{rs} and τ_{rg} are found from transport samples. However, if the transport samples are made with bedload traps, a sizable portion of the bed will need to be excavated to install the traps and it is advisable to sieve this sediment for future reference.

The gravel and sand fractions f_g and f_s are needed to calculate transport rates. Only one of these must be found; the other is given by $f_s + f_g = 1$. The sand content may be estimated from a visual survey of the reach upstream from the PXS. Calibrated visual estimates of f_s provide a relatively quick method with sufficient accuracy (Wilcock et al, 1996). Visual estimates of f_s should be calibrated for each field worker using pebble counts as a standard. Calibration pebble counts must be made within areas with uniform sand content. To find f_s for the reach upstream of the PXS, regions of similar f_s are mapped (enlarged copies of aerial photographs are convenient for this). The area of each uniform region is multiplied by the local f_s. These products are then summed and divided by the total bed area to give an area-weighted value of f_s.

Beyond the estimate of surface size distribution for hydraulic roughness, the primary observation of grain size required is f_s, if τ_{rg} and τ_{rs} are determined from transport observations. This is an important advantage of the two-fraction model. Because the visual estimation of f_s is relatively quick, it becomes possible to easily update the transport forecast if the bed size distribution is observed to change over time. Furthermore, because stream disturbance is commonly associated with an influx of fine sediment, these visual surveys provide a relatively simple way of monitoring an important channel impact.

Transport Observations

Transport observations are used to determine the values of τ_{rg} and τ_{rs}, which serve as surrogates for τ_{cg} and τ_{cs}. These measurements are best made at low flows producing transport rates close to the reference value. By happy coincidence, these are also the flows that can be measured with greatest accuracy and safety, provided that samples of sufficiently long duration are taken. In-bed sediment traps provide a means for collecting such samples.

Bedload traps may be conveniently made of plastic five gallon buckets, although other containers, such wooden boxes may also be used. It is important that the container be relatively deep compared to its width, in order to decrease the strength of eddies that might sweep sediment out of the trap. A standard five gallon plastic bucket has suitable dimensions. It is an advantage to have some means of removing the trap. Church et al. (1991) drove a one-ft. diameter pipe in the bed, into which they inserted 5 liter buckets. The entire bucket can then be removed. McArdell (1996, personal communication) inserted the buckets directly into the bed and then placed porous microfiber plastic sediment bags (commonly used to hold 100 pounds of sand) inside the buckets. Sample bags could be quickly removed and replaced with a fresh bag. The bags were secured to the top of the bucket with extra large rubber bands and a large painted cobble was placed inside the bag to hold it in place. Tight fitting or weighted lids are desirable to keep the traps from filling when not in use.

The number of traps used should be sufficient to give a representative sample across the entire active bed of the channel. In small channels (less than 15 m width), it is reasonable to consider covering half the channel width with traps.

To install the traps, the bed is excavated just to the depth at which the traps can placed with their upper edge level with the bed surface. To accomplish this, it is useful to survey the bed

before excavation. It is also useful to use a board to hold the upstream side of the excavation in place in order to minimize disturbance to the upstream bed. Once in place, the space around the traps is carefully backfilled in an attempt to recreate the undisturbed sediment bed, including reserving surface clasts for later placement on the bed surface. Transport observations from the initial transport event should be not be used.

During conditions close to incipient motion, the traps should be observed on a daily basis. More frequent observations are needed when the transport rate is larger. If the traps are filling in an hour or less, the transport rates will be well above the incipient motion condition needed to define τ_{rg} and τ_{rs} (although the samples may nonetheless be of interest!).

The sampled sediment should be weighed and sieved at one ϕ intervals. At a minimum, the total weight and the proportions greater than 8mm, between 2 and 8mm, and finer than 2mm should be determined. If weighing in the field is not possible, clasts larger than 8mm may be passed through a gravelometer and the number in each size class counted. A one-time calibration of number to weight for each size class should provide sufficient accuracy. Sediment finer than 8mm may be bagged and labeled and weighed later. The transport rate at each trap is the mass of sediment (either sand or gravel) in kg, divided by the cross-stream width of each trap and by the duration in seconds of the sample. The transport rates at each trap are multiplied by the width of bed that each trap represents. These subsectional transport rates are then summed and divided by the total active width to find the unit transport rates q_g and q_s for the entire the active channel. To determine τ_{rg} and τ_{rs}, it is best to obtain values of transport rate both larger and smaller than the reference transport rate, so that τ_{rg} and τ_{rs} can be found by interpolation on plots of q_g and q_g as a function of τ.

A major advantage of bedload traps is that they can sample for very long periods of time. This enhances the chances of sampling the onset of gravel motion, which tends to occur through rare, intermittent movements that can easily be missed by a hand-held sampler.

Transport Calculation

If no observations of transport are made, τ_{rg} and τ_{rs} are estimated using measured values of f_s, D_g and D_s in Figure 9.

When transport observations are made, the associated value of discharge Q is found from the stage-discharge relation for the PXS. The section mean velocity U is found by dividing Q by

the cross-sectional flow area at that stage. The corresponding value of skin friction τ is calculated from Eq. 20 using the observed values of S, D_{65} and U. Plots of q_g and q_s as a function of τ are made and τ_{rg} and τ_{rs} are found where the trend of the data intersect the reference line $q_b = 0.00001035\ \tau^{1.5}$ for q_b in kg/ms and τ in Pa (or, equivalently, where the trend of the data intersect $W^* = 0.002$ on a plot of W^* as a function of τ).

To calculate q_g and q_s at a specified discharge Q, the flow depth is found from the PXS rating curve, the corresponding flow cross-sectional area is found from the surveyed cross section, and the mean velocity is calculated as U = Q/A. This value of U is used with measured values of S and D_{65} to calculate τ from Eq. 20. This value of τ is used with values of f_s, f_g, τ_{rg} and τ_{rs} to calculate the gravel and sand transport rates from Eq. 16. The total gravel and sand transport through the section is found by multiplying q_g and q_s by the active width channel width.

Example, Illustrating the Relative Accuracy of the Two Options

An example serves to illustrate how transport forecasts are made. The example also provides an opportunity to illustrate the improved accuracy that may be achieved by directly estimating τ_{rg} and τ_{rs} from a small number of transport observations at small transport rates. The example will also demonstrate the weak dependence of the calculated transport rate on errors in estimating τ when values of τ_{ri} are found from transport observations.

The example uses fictitious values for simplicity, although they are based on flow and sediment conditions for the East Fork River. Assume that sand transport rate, discharge, and cross-sectional flow area have been determined at four different flows, as shown in the table below.

Q (cms)	A (m^2)	U (m/s)	q_s (kg/ms)
3.84	6.23	0.62	2.5E-05
4.79	7.20	0.67	8.7E-05
5.1	7.50	0.68	0.00035
5.75	8.11	0.71	0.0009

Flow velocity is calculated as Q/A. The flow is found to be uniform and a field survey established that the water surface slope is equal to the mean bed slope of 0.0007. D_{65} from a pebble count within one channel width of the PXS is 3.2 mm, so k_s is 6.4 mm. The observed values of q_s and Q are graphed in Figure 13.a. In part b of the figure, the same transport rates are plotted as a function τ, which is calculated using Eq. 20. Also shown in Figure 13.b is a second case, corresponding to k_s = 25.6 mm, chosen to be much larger in order to demonstrate the influence of error in k_s on estimates of τ and q_s. The second k_s value is four times the first. As a result, the second set of τ values is 1.41 times the first ($1.41 = 4^{0.25}$, from Eq. 20). The plot in Figure 13b is used to find τ_{rs}, which is the value of τ where the transport data intersect the reference transport line. For the larger k_s case, the value of τ_{rs} is approximately 1.4 times larger than the first case.

Values of q_s calculated for a range of Q are given in Figure 13.a. Here, flow depth and flow area are found for a specified value of Q using the stage-discharge and stage-area curves for the PXS. U is then calculated and τ found using Eq. 20. When the two alternative values of k_s and τ_{rs} are used to estimate transport rates with Eq. 16, the difference between the two transport estimates is much smaller than the apparent difference evident on Figure 13.b. At small values of τ/τ_r, the term $(1 - \tau_r/\tau)^{4.5}$ in Eq. 16 dominates and the two transport estimates are essentially the same. This is because the difference in estimated τ_{rs} is almost identical to the difference in calculated τ, so the ratios τ/τ_{rs} are nearly identical for the two cases. At large values of τ/τ_r, the term $(\tau)^{1.5}$ in Eq. 16 dominates, so the ratio of the two transport estimates increases with τ/τ_r, but will not exceed the ratio of the two values of τ raised to the 3/2 power ($1.41^{1.5} = 1.68$).

The influence of uncertainty in τ_{ri} on calculated q_s is much larger if τ_{ri} is estimated independently. Figure 13.a shows q_s calculated using values of τ_r that are two times larger and smaller than the value chosen using k_s = 6.4mm in Figure 13.b. A factor of two difference in τ_r is plausible. For example, it is the difference between the observed value of τ^*_{rs} for the East Fork River and a value of 0.04 that might be estimated for a river with 59% sand. The difference in calculated q_s for the different values of τ_r is very large, particularly at small values of τ/τ_{ri}. This example also provides a more general illustration of the influence of uncertainty in τ (or τ_r) on error in calculating transport rates. The uncertainty arises from many sources, including spatial variability in τ and transport, inaccurate drag partitioning, error in measurements. The steep nature of the transport function magnifies these errors in τ, and represents the largest source of error in

estimating transport rates in the field. Reducing this error is the basic motivation for determining incipient motion conditions directly from transport observations.

Acknowledgments

This work was supported by the National Stream Systems Technology Center, under Partnership Agreement 28-CCS5-019 between the Johns Hopkins University and The U.S. Forest Service Rocky Mountain Forest and Range Experiment Station. The support and patience of Larry Schmidt and John Potyondy is much appreciated. Bill Emmett, Roger Kuhnle, Tom Lisle, and Bob Milhous freely provided data, advice, and stimulating discussion regarding their field data sets, without which the analysis conducted here would not have been possible.

References

Ackers, P., and W.R. White, Sediment transport: new approach and analysis, *J. Hydraul. Div., Amer. Soc. Civil Eng.*, 99(HY11), 2041-2060, 1973.

Andrews, E.D., Entrainment of gravel from naturally sorted riverbed material, *Geol. Soc. Amer. Bull.*, 94, 1225-1231, 1983.

Bagnold, R.A., The flow of cohesionless grains in fluids, *Philosophical Trans. Royal Society London* A, 249, No. 964, 1956.

Beschta, R. L., Conceptual models of sediment transport in streams, in Thorne, C.R., J.C. Bathurst, and R.D. Hey (eds.), *Sediment Transport in Gravel-bed Rivers*, John Wiley & Sons, 1987.

Beschta, R. L. and W. L. Jackson. The intrusion of fine sediments into a stable gravel bed, *Journal of the Fisheries Research Board of Canada*, 36, 204-210, 1979.

Bowie, A.J., Comparison of "n" values in natural and dredged channels, in Wang, S.Y. (ed.), *Proceedings, Int. Symp. on Sediment Transport Modeling*, New Orleans, 1989.

Church, M.A., D.G. McLean, and J.F. Wolcott, River bed gravels: sampling and analysis, in Thorne, C.R., J.C. Bathurst, and R.D. Hey (eds.), *Sediment Transport in Gravel-bed Rivers*, John Wiley & Sons, 1987.

Church, M., J. F. Wolcott, and W. K. Fletcher, A test of equal mobility in fluvial sediment transport: behavior of the sand fraction, *Water Res. Res.*, 27(11), 2941-2951, 1991.

Diplas, P., and G. Parker, Pollution of gravel spawning grounds due to fine sediment, *Proj. Report No. 240*, St. Anthony Falls Hydr. Lab., Univ. Minnesota, 1985.

Einstein, H.A., The bedload function for sediment transport in open channel flows, *Tech. Bull. 1026*, U.S. Dep. of Agric., Soil Conserv. Serv., Washington, D.C., Sept. 1950.

Emmett, W.W., A field calibration of the sediment-trapping characteristics of the Helley-Smith bedload sampler, USGS *Professional Paper* 1139, 1980.

Emmett, W.W., R.H. Myrick, and H.A. Martinson, Hydraulic and sediment-transport data, East Fork River, Wyoming, 1978. USGS *Open-File Report* 85-486, 1985.

Emmett, W.W., R.H. Myrick, and R.H. Meade, Field data describing the movement and storage of sediment in the East Fork River, Wyoming, Part 1. River hydraulics and sediment transport, 1979. USGS *Open-File Report* 80-1189, 1980.

Engelund, F., Closure to "Hydraulic resistance of alluvial streams", *J. Hydraul. Div., Am. Soc. Civil Eng.*, 93(HY4), 287-296, 1967.

Ferguson, R.I., K.L. Prestegaard, and P.J. Ashworth, Influence of sand on hydraulics and gravel transport in a braided gravel bed river: *Water Resources Research*, v. 25, p. 635-643, 1989.

Harrelson, C.C., C. L. Rawlins, and J.P. Potyondy, *Stream channel reference sites: an illustrated guide to field techniques*. Gen. Tech. Rep. RM-245. Fort Collins, CO: U.S. Dept. of Agriculture, Forest Service, Rocky Mountain Forest and Range Experiment Station. 61 p., 1994.

Henderson, F. M., *Open Channel Flow*. MacMillan, 522 p., 1969.

Ikeda. H. and F. Iseya, Experimental study of heterogeneous sediment transport, *Environmental Research Center Papers, No. 12*, Univ. of Tsukuba, Japan, 1988.

Iseya, F. and H. Ikeda, Pulsations in bedload transport rates induced by longitudinal sediment sorting: a flume study using sand and gravel mixtures, *Geograf. Ann.*, 12-27, 1987.

Jackson, W. L., and R. L. Beschta, A model of two-phase bedload transport in an Oregon coast range stream, *Earth Surface Processes and Landforms*, 9, 517-527, 1982.

Kuhnle, R.A, Fractional transport rates of bedload on Goodwin Creek, in Billi, P., Hey, R.D., Thorne, C.R., and Tacconi, P., (eds.), *Dynamics of Gravel-bed Rivers*, John Wiley & Sons, 1992.

Kuhnle, R.A. and A.J. Bowie, Loop rating curves from Goodwin Creek, *Proc.* , ASCE Hydraulic Engineering Conf., Baltimore, 1994.

Leopold L.B. and W.W. Emmett, in review, Bedload and river hydraulics—Inferences from the East Fork River, Wyoming, USGS *Professional Paper* in prep.

Leopold, L.B., Sediment size that determines channel morphology, in *Dynamics of Gravel-bed Rivers*, edited by P. Billi, R.D. Hey, C.R. Thorne, and P. Tacconi, John Wiley and Sons, New York, 1992.

Lisle, T., Stabilization of a gravel channel by large streamside obstructions and bedrock bends, Jacoby Creek, northwestern California, *GSA Bulletin*, 97:999-1011, 1986.

Lisle, T., Sediment transport and resulting deposition in spawning gravels, north coastal California, *Water Resources Research*, 25(6):1303-1319, 1989.

Meyer-Peter, E., and R. Müller, Formulation for bed load transport, *Proc. 2nd Congress*, Int. Assoc. Hydr. Res., Stockholm, Sweden, pp. 39-64, 1948.

Milhous, R.T., Sediment transport in a gravel-bottomed stream, Ph.D. thesis, Oregon State Univ., Corvallis, 1973.

Nelson, J.M., W.W. Emmett, and J.D. Smith, Flow and sediment transport in rough channels, in *Proc. of the Fifth Interagency Sedimentation Conference*, Las Vegas, Vol. 2, Section 4, pp. 55-62, 1991.

Paola, C. and R. Seal, Grain size patchiness as a cause of selective deposition and downstream fining, *Water Res. Res.*, , 1995.

Parker, G., Hydraulic geometry of active gravel rivers, *J. Hydraul. Div.*, Am. Soc. Civ. Eng., 105(HY9), 1185-1201, 1979.

Parker, G., and P. C. Klingeman, On why gravel bed streams are paved, *Water Res. Res.*, 18, 1409-1423, 1982a.

Parker, G., P.C. Klingeman, and D.L. McLean, Bedload and size distribution in paved gravel-bed streams, *J. Hydraul. Div.*, Am. Soc. Civ. Eng., 108(HY4), 544-571, 1982b.

Whiting, P. J. and W. E. Dietrich, Boundary shear stress and roughness over mobile alluvial beds, *J. Hydraul. Eng.*, 116(12), 1495-1511, 1990.

Wiberg, P. L. and J. D. Smith, Velocity distribution and bed roughness in steep streams, *Water Resources Research*, 27(5), 825-838, 1991.

Wilcock, P. R., Methods for estimating the critical shear stress of individual fractions in mixed-size sediment, *Water Res. Res.*, 24(7), 1127-1135, 1988.

Wilcock, P. R., Experimental investigation of the effect of mixture properties on transport dynamics. In Billi, P., R. D. Hey, C. R. Thorne, and P. Tacconi (eds.), *Dynamics of Gravel-bed Rivers*, John Wiley & Sons., pp. 109-139, 1992.

Wilcock, P. R., The critical shear stress of natural sediments, *J. Hydr. Engineering*, 119(4), 491-505, 1993.

Wilcock, P.R., The components of fractional transport rate, *Water Resources Research*, 33(1):247-258, 1997.

Wilcock, P.R., Kondolf, G.M., Matthews, W.V.G., and Barta, A.F., 1996. Specification of sediment maintenance flows for a large gravel-bed river, *Water Resources Research*, 32(9):2911-2921, 1996.

Wilcock, P.R. and McArdell, B.W., Surface-based fractional transport rates: mobilization thresholds and partial transport of a sand-gravel sediment, *Water Resources Research*, 29(4):1297-1312, 1993.

Wilcock, P.R., and McArdell, B.W., Partial transport of a sand-gravel sediment, *Water Resources Research* 33(1):233-245, 1997.

Wilcock, P.R., and J.B. Southard, Bed-load transport of mixed-size sediment: fractional transport rates, bed forms, and the development of a coarse bed-surface layer, *Water Resources Research*, v. 25, 1629-1641, 1989.

Wilcox, M.S, C.A. Troendle, and J.M. Nankervis, Bedload transported in gravelbed streams in Wyoming, Sixth Interagency Sedimentation Conference, Las Vegas, 1996

Yalin, M.S., *River Mechanics*, Pergammon Press, 219 p., 1992.

Table 1. Summary Table of the Flow and Sediment Characteristics of the Five Cases

	Bed Slope	Channel Width* (m)	Bankfull Discharge (cms)		Discharge (cms)	Flow Depth (m)	Mean Velocity (m/s)	Transport Rate (kg/m/s)	Bed D50 (mm)	Bed D65 (mm)	Bed D90 (mm)	Sand/gravel Boundary (mm)		fi	Di (mm)	Source
East Fork River, WY	0.0007	19	20	min	3.44	0.39	0.61	0.0003	1.2	3.2	28	2.00	sand	0.59	0.6	Leopold and Emmett (1997)
		(14.6)		max	41.5	2.01	1.41	0.29					gravel	0.41	12.0	Emmett (1980)
Goodwin Creek, MS	0.0033	25		min	1.5	0.6	0.25	0.0002	8.3	15.1	30	2.00	sand	0.34	0.6	Kuhnle (1992)
		(20.7)		max	40	2.2	1.4	3.0					gravel	0.66	16.0	
Jacoby Creek, CA	0.0063	17.2	19.6	min	0.60	0.15	0.61	0.000032	20	35	88	2.00	sand	0.10	1.4	Lisle (1986, 1989)
		(12.0)		max	39.6	0.86	40	0.413					gravel	0.90	24.0	
Oak Creek, OR	0.014	6		min	0.54	0.2	0.68	0.0000084	20	32	65	2.38	sand	0.15	1.2	Milhous (1973)
		(3.7)		max	3.4	0.6	1.16	0.111					gravel	0.85	26.0	
Bed of Many Colors (lab)	varies	0.6	-	min	0.0173	0.09	0.26	0.0000023	5.2	11.8	30	2.00	sand	0.34	0.5	Wilcock and McArdell (1993)
				max	0.0570	0.11	1.1	0.572					gravel	0.66	13.0	

Some values of channel geometry and hydraulics are approximate.

* Channel Width: approx top width (bottom width)

List of Figures

Figure 1 Schematic illustration of the accuracy/cost tradeoff for predicting transport from transport samples alone, from a transport formula alone, and from a combination of the two approaches in which a few transport samples are used to improve the accuracy of the predicted transport.

Figure 2 Grain-size distributions for the annual bed-material load and the river bed subsurface, Coon Creek, Wyoming (Wilcox et al., 1996).

Figure 3 Flume demonstration of the influence of sand content on the transport of sand and gravel (Ikeda and Iseya, 1988).

Figure 4 Grain-size histograms of the five sediment beds.

Figure 5 Cumulative curves of the grain-size distributions of the five sediment beds.

Figure 6 Bed load transport as a function of discharge for the East Fork River. 118 individual samples were grouped into 18. Data of Emmett (1980) and Emmett et al. (1980, 1985).

Figure 7 Bed load transport as a function of discharge for Jacoby Creek. 105 individual samples were grouped into 15. Largest group represents overbank flow. Smallest three groups include small sample size. Data of Lisle (1989).

Figure 8 Fractional transport rate of sand and gravel as a function of skin friction shear stress.

Figure 9 Dimensionless reference shear stress as a function of sand content.

Figure 10 Influence of flow and transport parameters on a similarity collapse of transport rates. The Parker-Einstein transport function is plotted for 32mm gravel and 1mm sand. Two values of critical shear stress are used for the sand.

Figure 11 Similarity collapse of gravel and sand transport rates.

Figure 12 Similarity collapse of gravel and sand transport rates. Same as Figure 11, with sand and gravel shown on same plot.

Figure 13 Example of the calculation of sand and gravel transport rates, illustrating the effect on predicted transport of error in reference shear stress and hydraulic roughness.

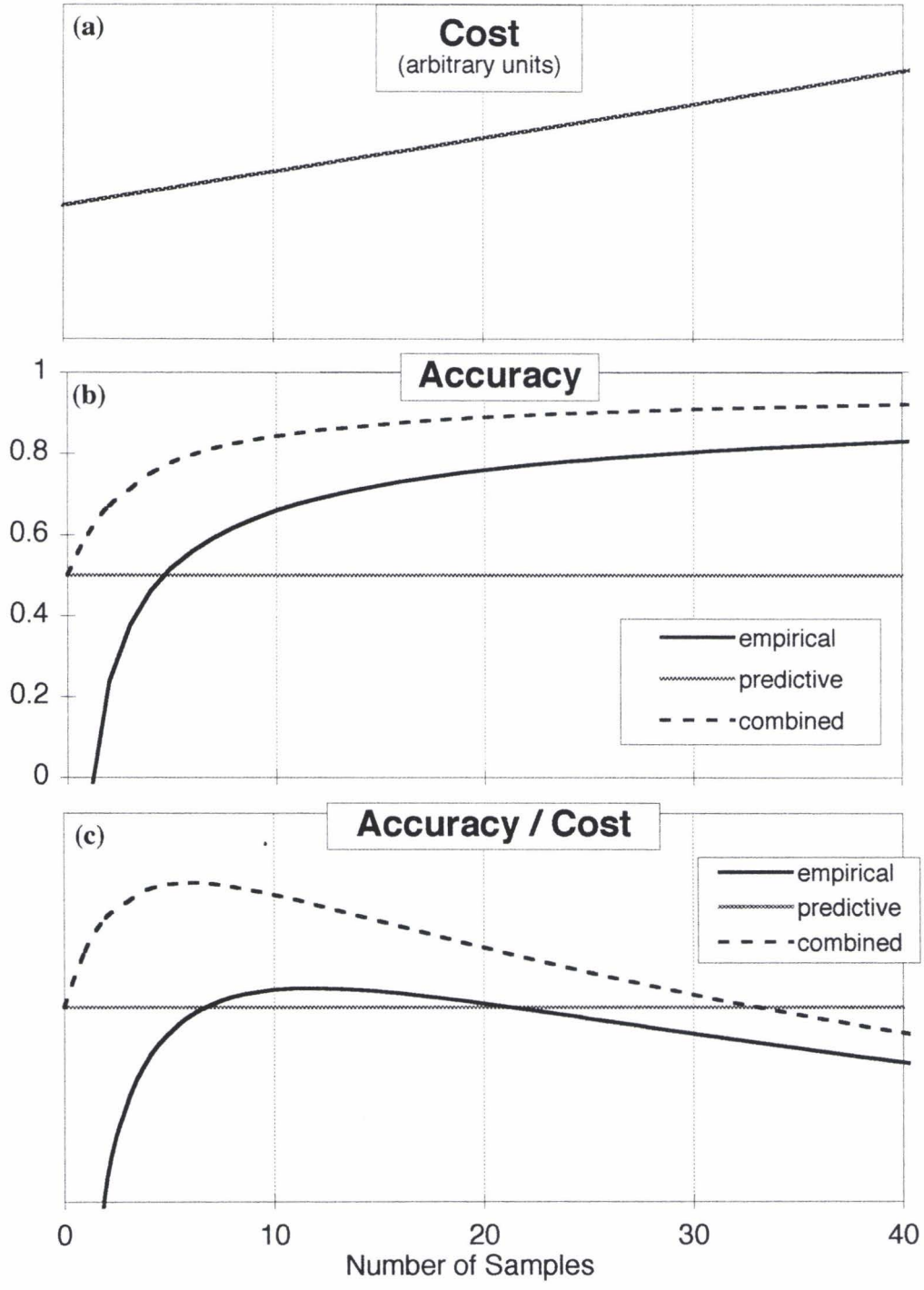

Figure 1. Schematic illustration of the accuracy/cost tradeoff for predicting transport from transport samples alone (empirical), from a transport formula alone (predictive), and from a combination of the two approaches in which a few transport samples are used to improve the accuracy of the predicted transport (combined). Predictive accuracy is assumed to be 0.5. Accuracy for the other two methods increases with the square root of sample number and depends on the sample standard deviation for the transport observations, which is assumed to be equal in magnitude to the measured transport rate.

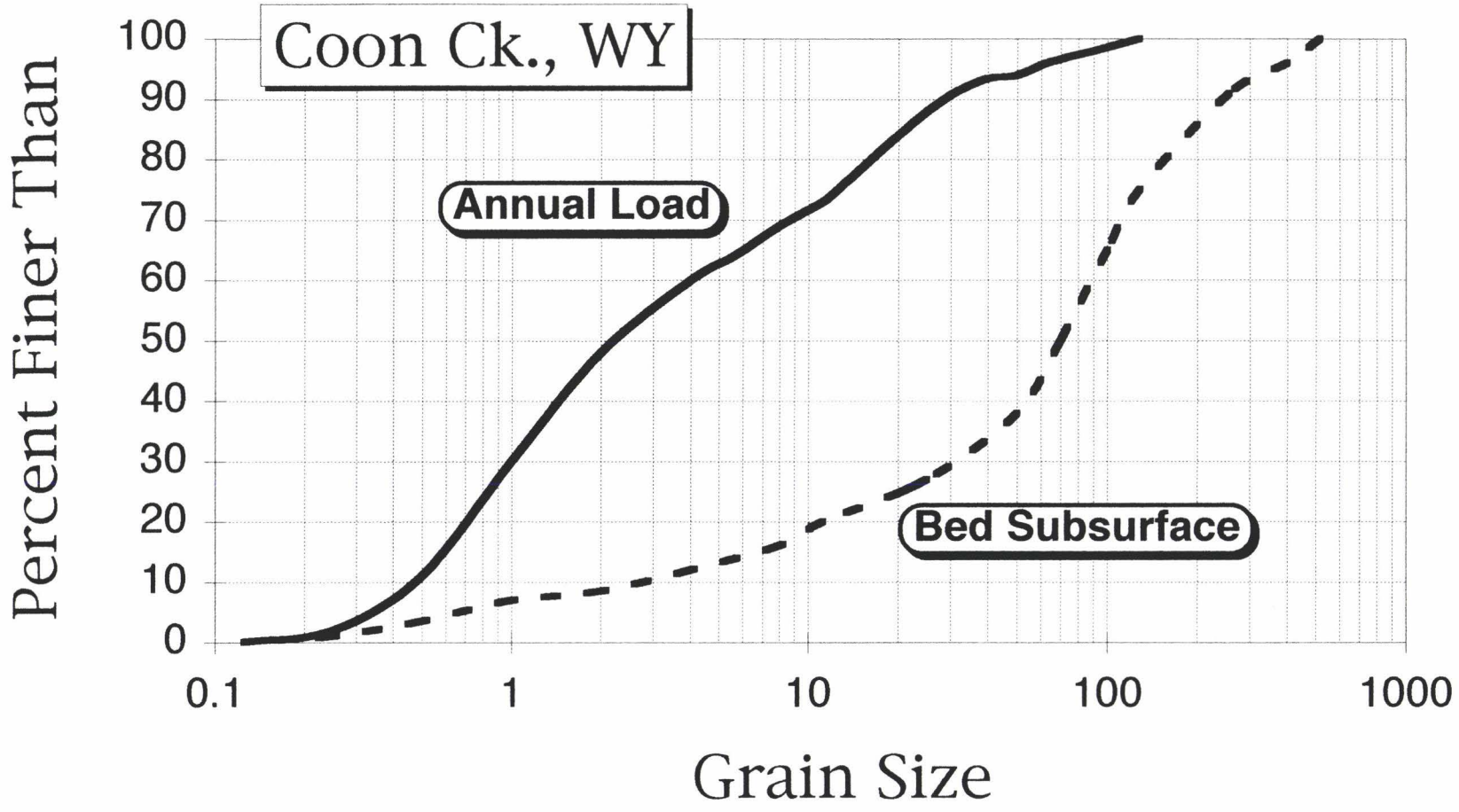

Figure 2. Grain-size distributions for the annual bed-material load and the river bed subsurface, Coon Creek, Wyoming (Wilcox et al., 1996).

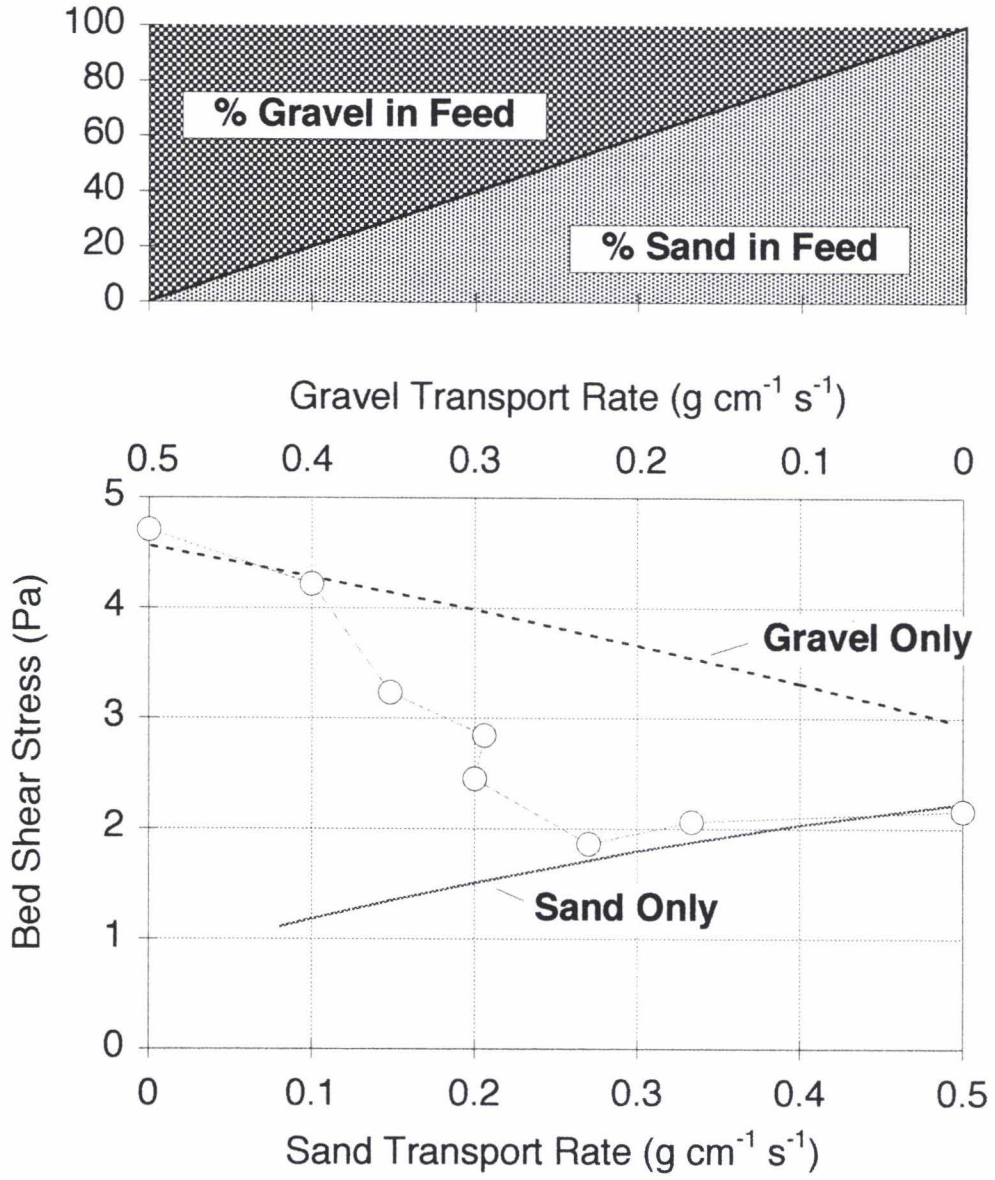

Figure 3. Flume demonstration of the influence of sand content on the transport of sand and gravel (Ikeda and Iseya, 1988)

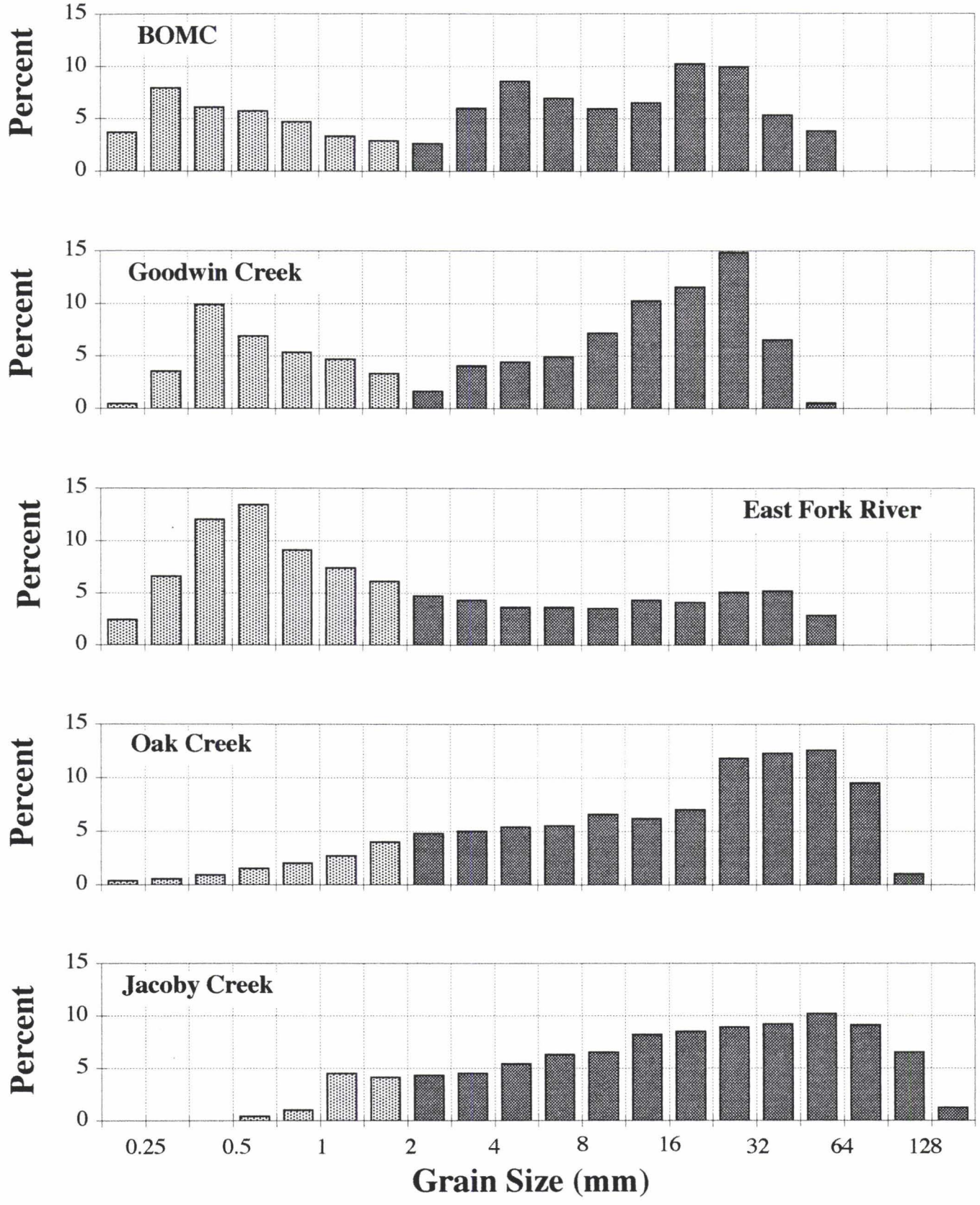

Figure 4 Grain-size histograms of the five sediment beds

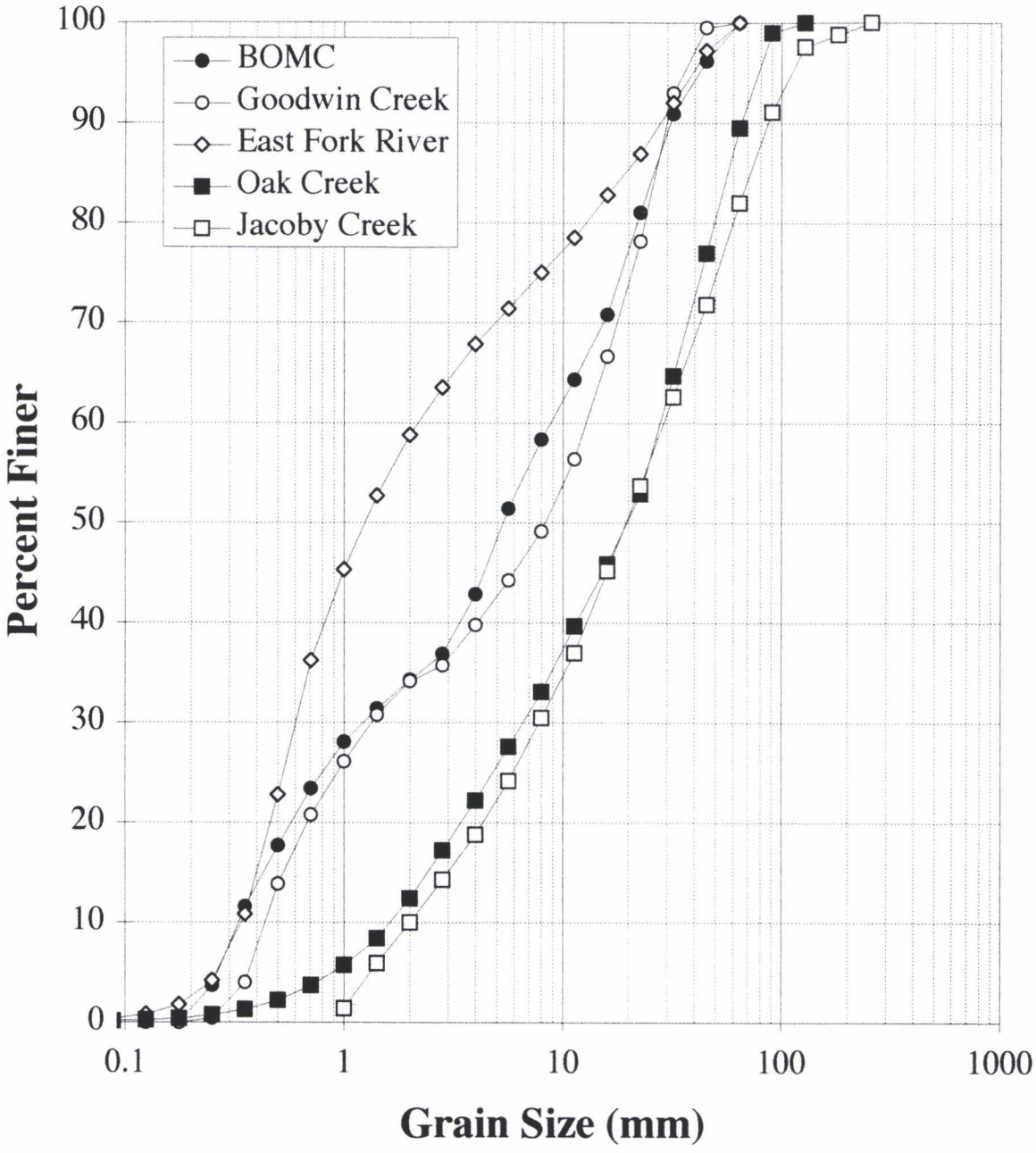

Figure 5. Cumulative curves for the grain-size distribution of the five sediments.

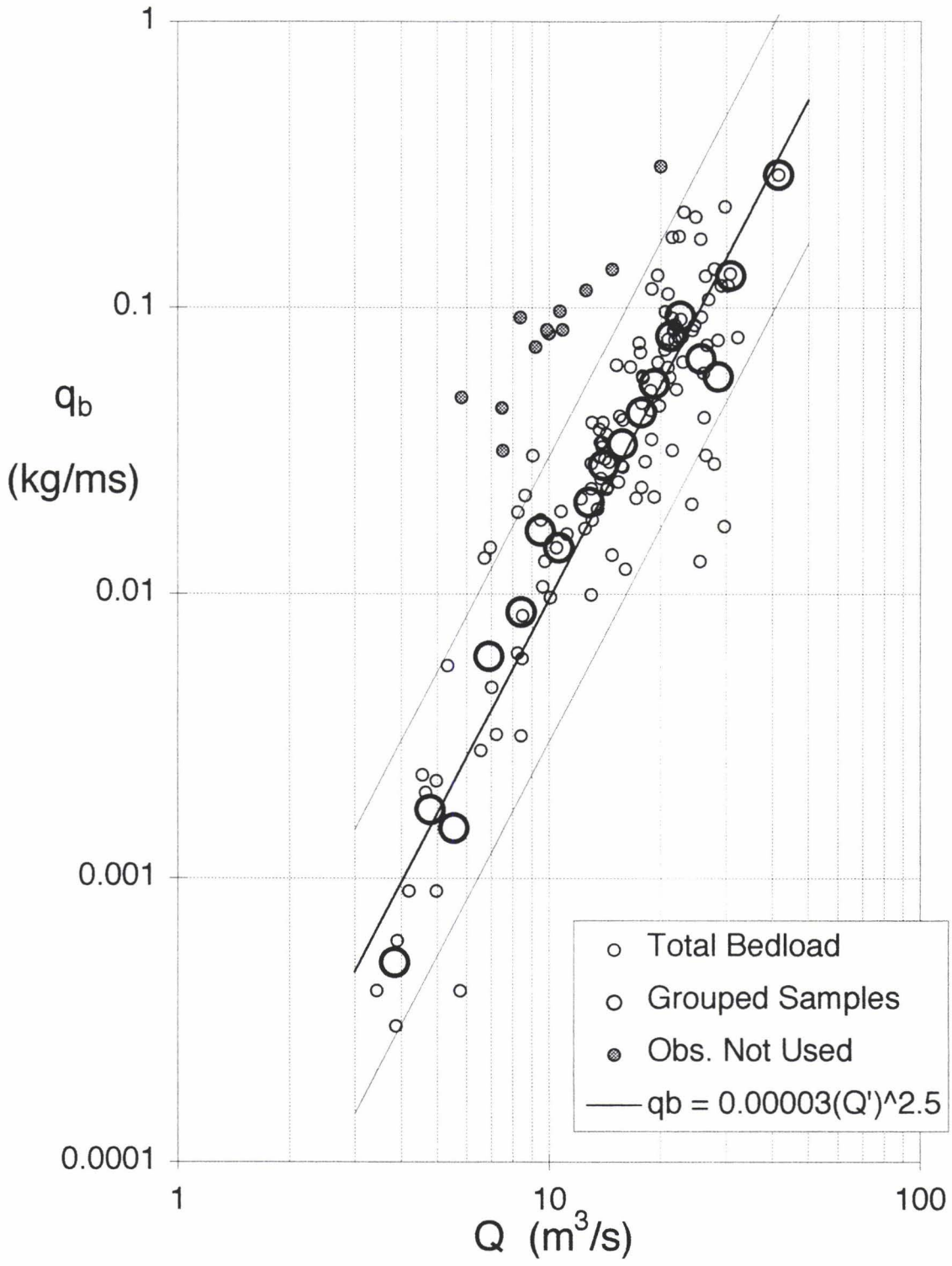

Figure 6. Bed-load transport rate as a function of discharge for the East Fork River. 118 samples were grouped into 18. Data of Emmett (1980), Emmett et al. (1980, 1985).

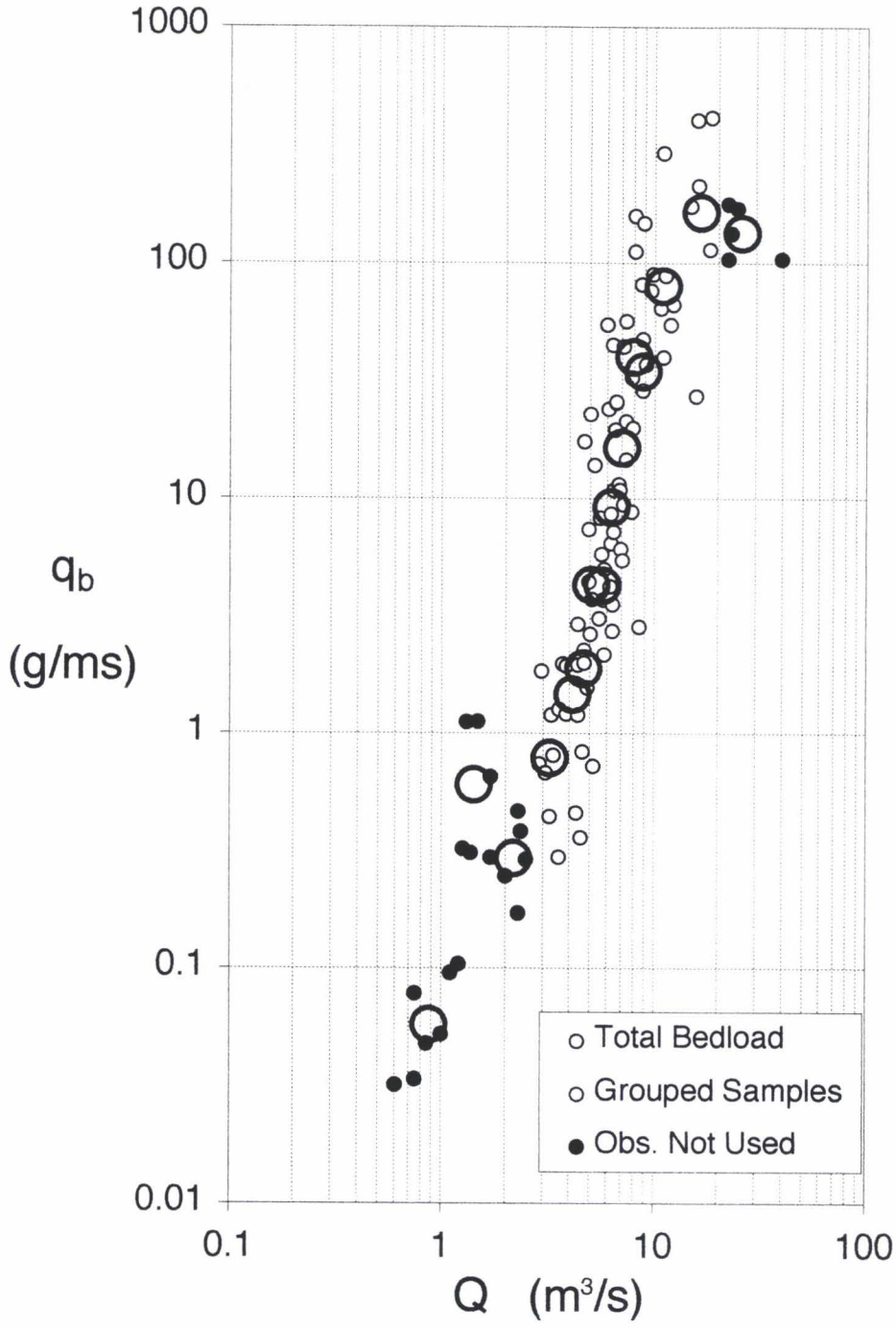

Figure 7. Bed load transport as a function of discharge for Jacoby Creek. 105 samples were grouped into 15. Largest group is for overbank flow. Smallest three groups have very small sample size. Data of Lisle (1989).

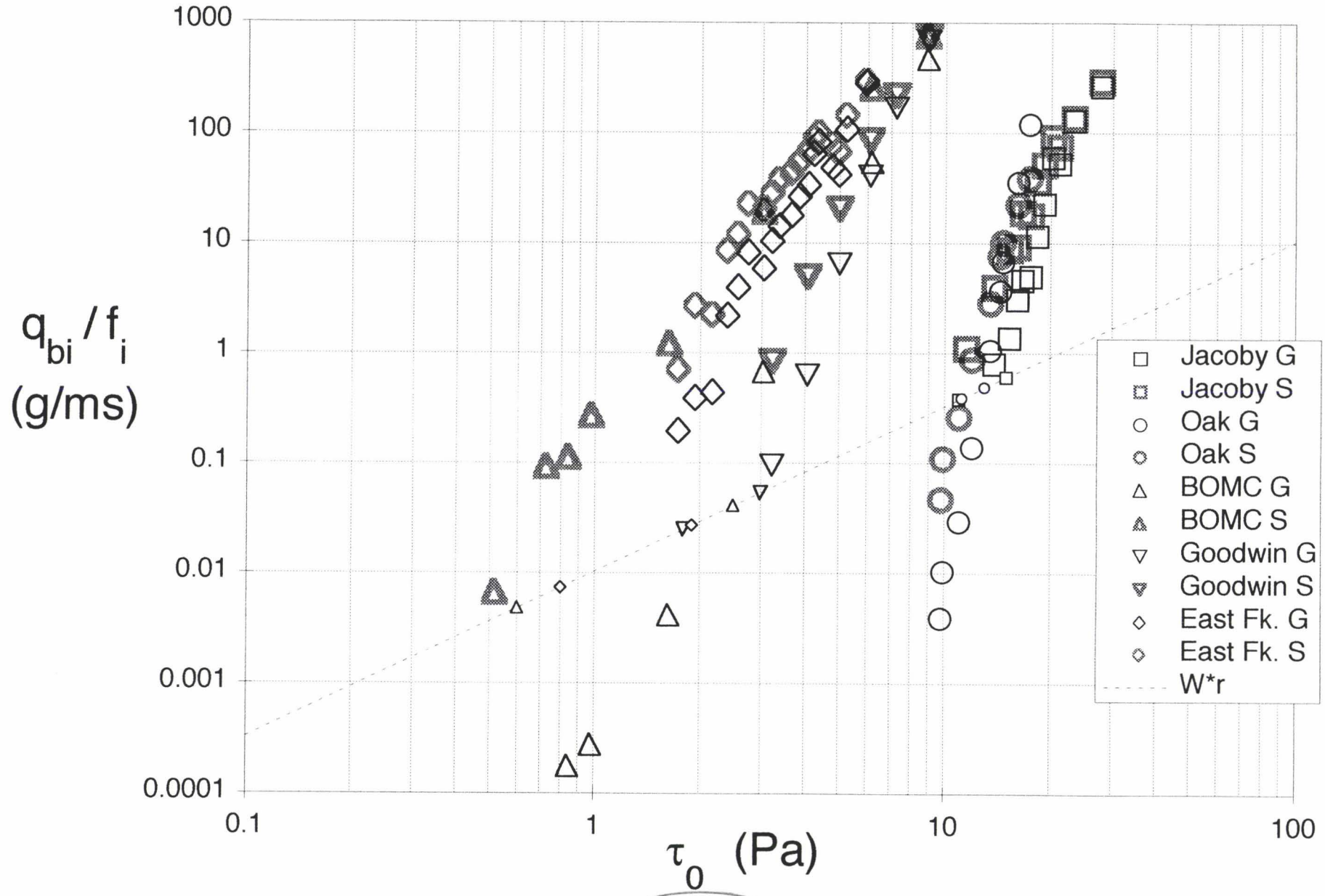

Figure 8. Fractional transport rate of sand and gravel as a function of skin friction shear stress.

(a)

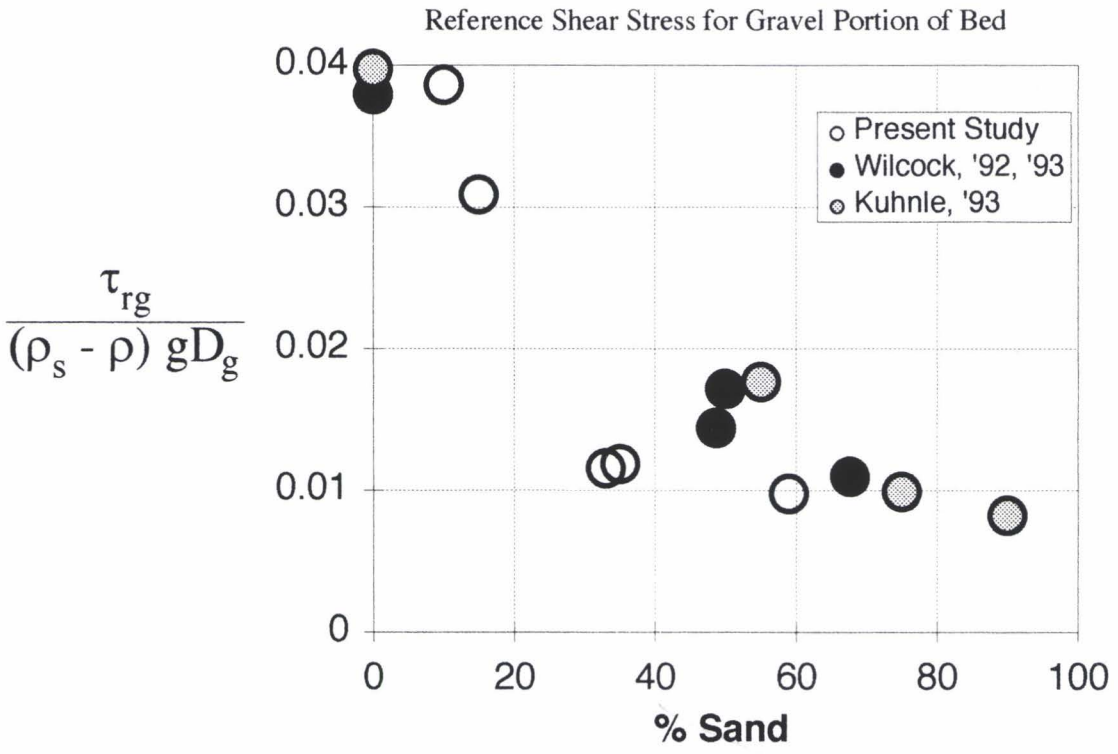

(b)

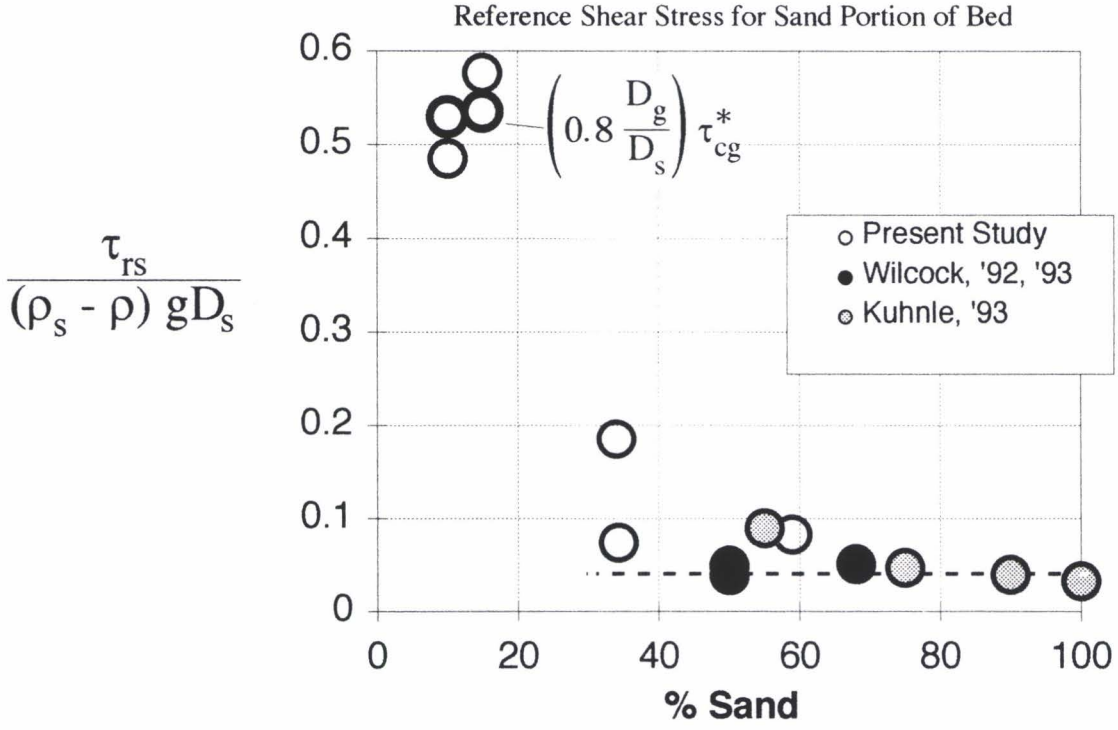

Figure 9 Dimensionless reference shear stress as a function of sand content.

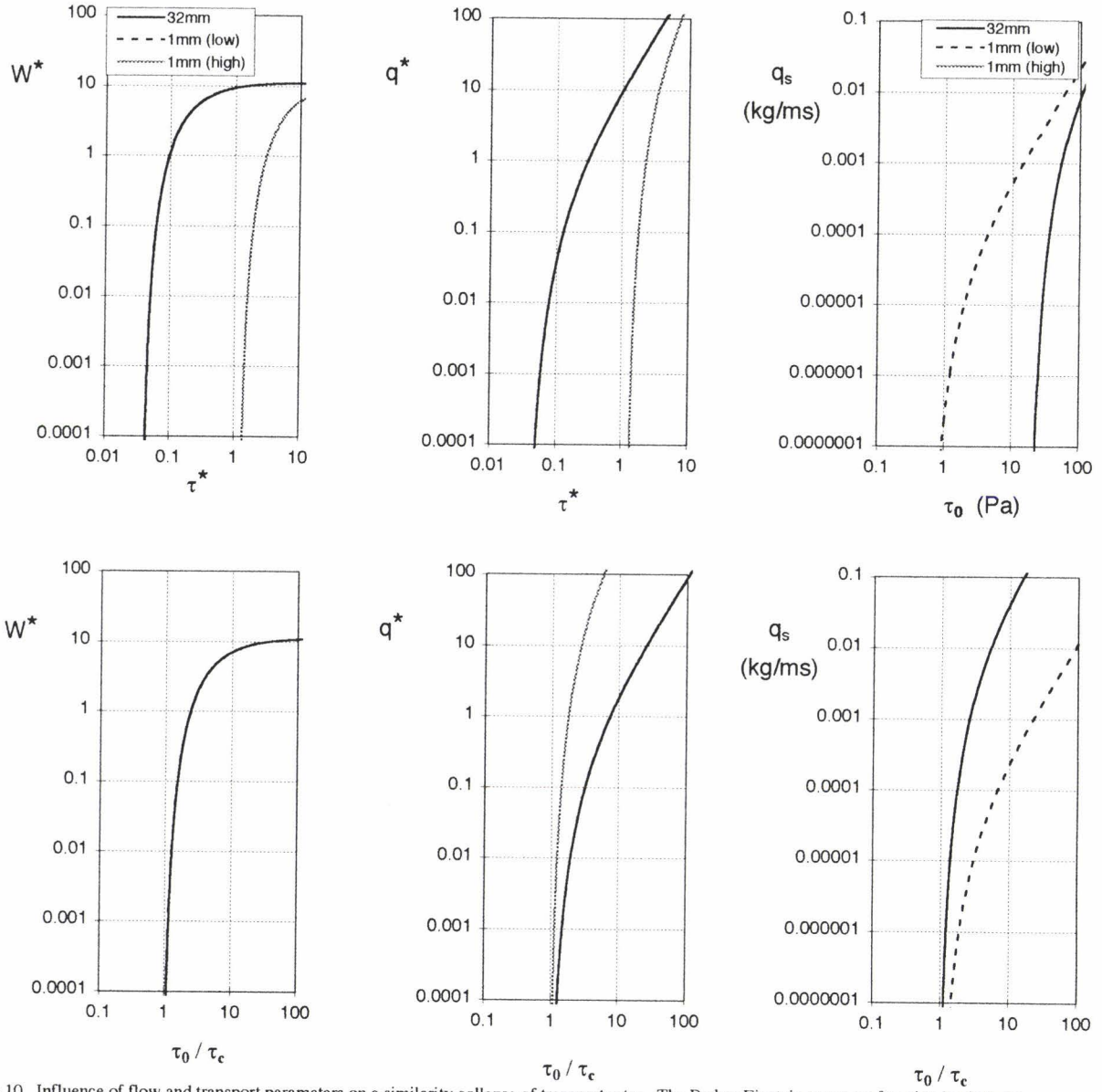

Figure 10. Influence of flow and transport parameters on a similarity collapse of transport rates. The Parker-Einstein transport function is plotted for 32mm gravel and 1mm sand. Two values of critical shear stress are used for the sand. See text for further discussion.

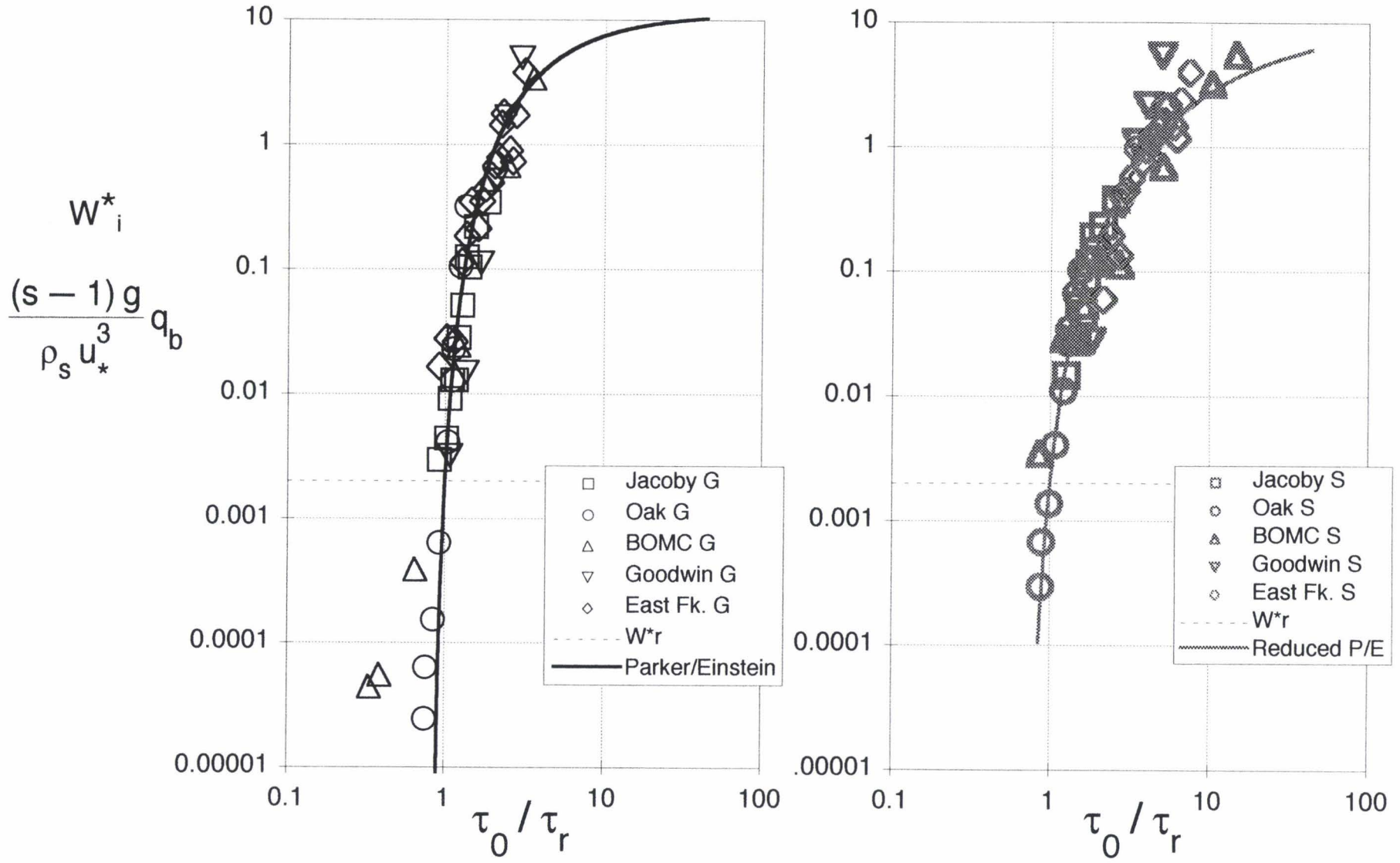

Figure 11. Similarity collapse of gravel and sand transport rates.

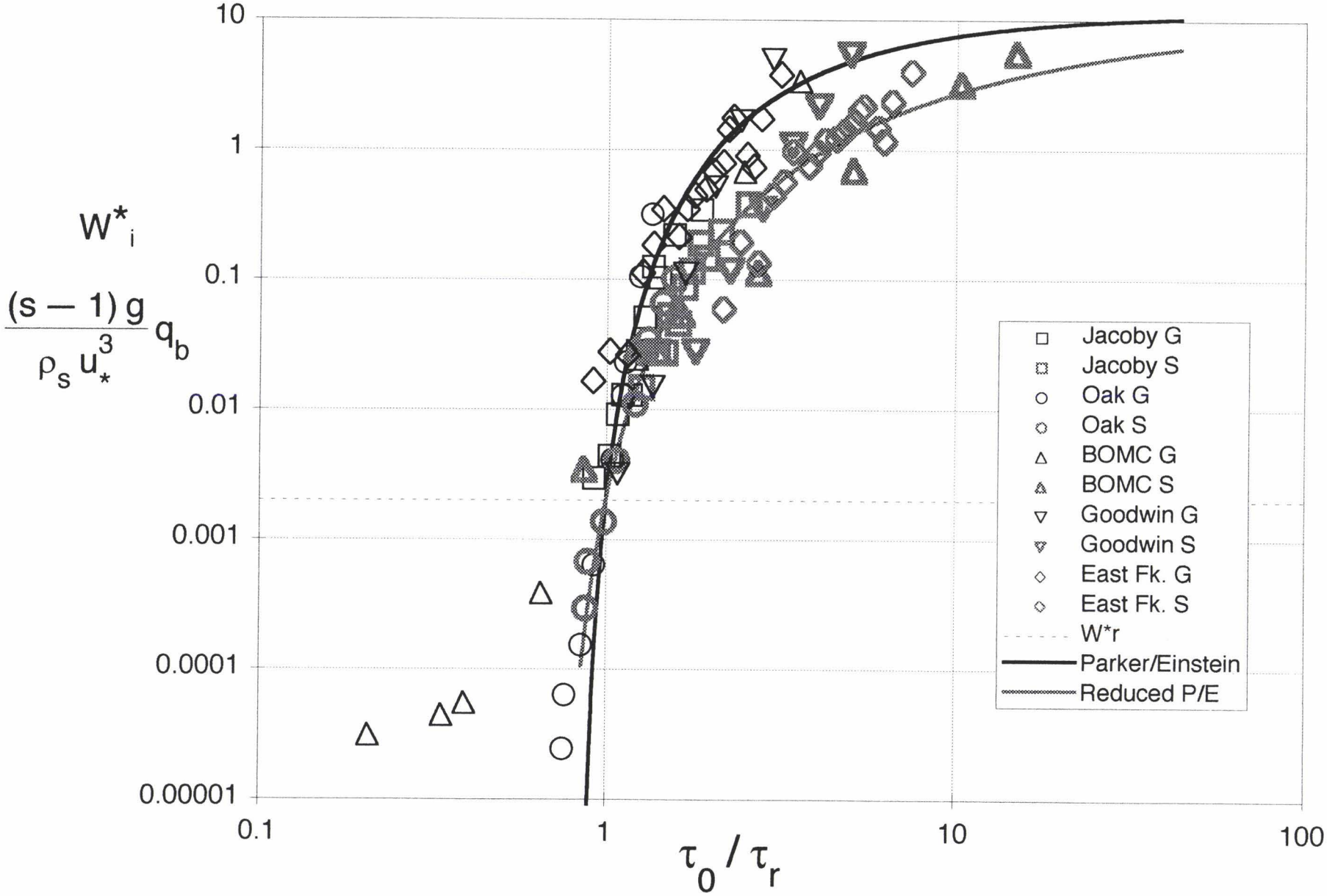

Figure 12. Similarity collapse of gravel and sand transport rates. Same is Figure 11, but with sand and gravel on same plot.

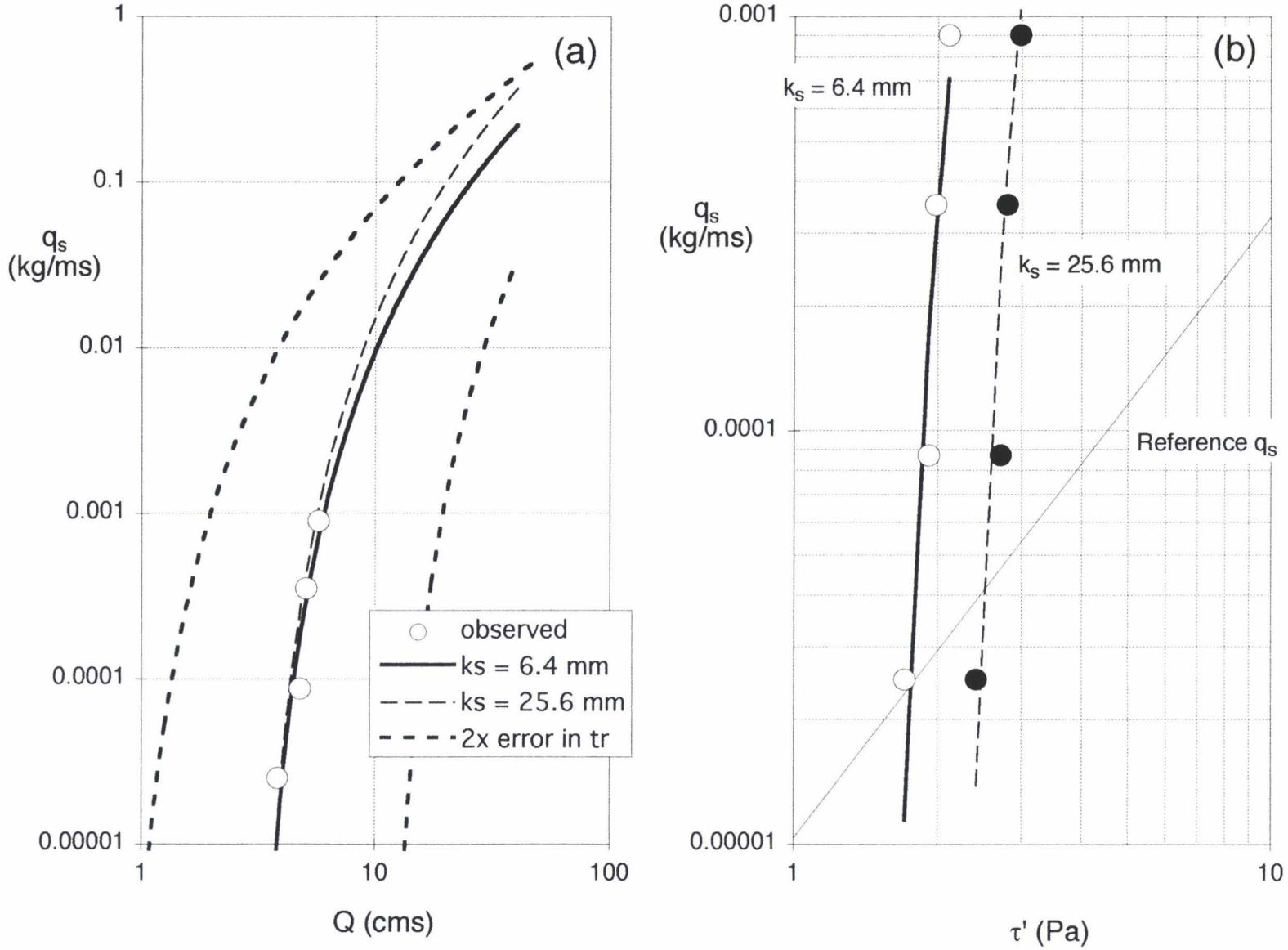

Figure 13. Example of the calculation of sand and gravel transport rates, illustrating the effect on predicted transport of error in reference shear stress and hydraulic roughness.

Produced by JHU Design and Publications